Chapter 2
Mathematical Models of Flow in Porous Media

In this chapter a general model for the two-phase fluid flow in porous media is presented, together with its simplified form, known as the Richards equation, which is applicable (under specific assumptions) to describe water flow in the vadose zone. In each case the governing equations are formulated at the Darcy scale, using the capillary pressure–saturation relationship and an empirical extension of the Darcy equation for the multiphase flow. The validity of these concepts, and the models based on them, is a subject of ongoing scientific debate, due to unclear connections between the pore-scale and Darcy-scale physical quantities, e.g. [25, 29, 32, 56, 66, 88]. Nevertheless, the models described here can be used to simulate many practical cases of multiphase flow in the subsurface with sufficient accuracy, e.g. [17, 31]. Therefore, they have been assumed as the starting point for the analysis presented in this work.

The two-phase flow model considered here is based on the following assumptions:

1. Pore air and pore water are single-component fluids.
2. Mass transfers between the fluids, i.e. the dissolution of air in water and the evaporation of water, are neglected.
3. The flow is isothermal.
4. Both fluid phases are barotropic, i.e. each phase density depends only on the pressure in the respective phase.
5. The solid phase is homogeneous, materially incompressible and does not react with the pore fluids.
6. The solid skeleton is rigid.
7. The flow of each fluid can be described by the extended Darcy formula including the relative permeability coefficient.

Additional assumptions underlying the Richards equation are discussed in Sect. 2.2.2. Fluid compressibility and soil skeleton deformation are not essential for the range of problems considered in this book. However, fluid compressibility is included in order to retain parabolic character of the governing equations for single phase flow. For a description of more comprehensive modeling approaches, which take into account the deformation of porous medium, see e.g. [20, 24, 47, 59, 70]. In the following

sections the key components of the model are briefly outlined, based to a large extent on the works [31, 33, 63].

2.1 Fundamental Concepts

2.1.1 Wettability and Capillarity

When two fluids are present in the pore space, one of them is preferentially attracted by the surface of the solid skeleton. It is called the wetting fluid (or phase), while the other fluid phase is called non-wetting. Here we consider only hydrophilic porous media, showing greater affinity to water than to air, which are more widespread in nature [33]. In the following the term wetting phase will be used as a synonym for water and the term non-wetting phase—as a synonym for air.

Immiscible fluids are separated by a well defined interface, which, if observed at a scale much larger than the molecule size, can be considered infinitely thin. Since the cohesion between fluid molecules at one side of the interface is different from that at the other side, the interface is characterized by some surface energy (or surface tension), which is a measure of the forces that must be overcome to change its shape. One consequence of the existence of the surface tension is the difference in the equilibrium pressures of air and water, separated by a curved interface, due to unbalanced tangential forces at the dividing surface. The pressure drop between the air and water phases can be calculated from the Laplace equation [63]:

$$\Delta p = p_{\mathrm{a}} - p_{\mathrm{w}} = \sigma_{\mathrm{aw}} \left(\frac{1}{r_{\mathrm{c}1}} + \frac{1}{r_{\mathrm{c}2}} \right), \tag{2.1}$$

where the subscripts a and w denote the air and water phases, respectively, σ_{aw} is the surface tension of the air–water interface, and $r_{\mathrm{c}1}$ and $r_{\mathrm{c}2}$ are the main curvature radii of the interface. The value of air-water surface tension at the temperature of $20\,^\circ\mathrm{C}$ is equal to $0.0726\ \mathrm{N\,m^{-1}}$ and decreases with increasing temperature [63]. The pressure is always smaller in the fluid occupying the concave side of the interface. In the absence of any external forces, the interface of a droplet of one fluid contained in another fluid tends to assume a spherical shape, which minimizes the surface energy.

In the presence of a solid surface the shape of the interface is determined by the relative magnitude of the surface tensions between all three phases, Fig. 2.1a:

$$\sigma_{\mathrm{aw}} \cos \psi = \sigma_{\mathrm{sa}} - \sigma_{\mathrm{sw}} , \tag{2.2}$$

where σ_{sa} and σ_{sw} are the values of the surface tension between the solid phase and air and water, respectively, and ψ is called the wetting angle. For a perfectly wetting fluid, $\psi = 0^\circ$, i.e. the fluid tends to spread evenly over the whole solid surface. For
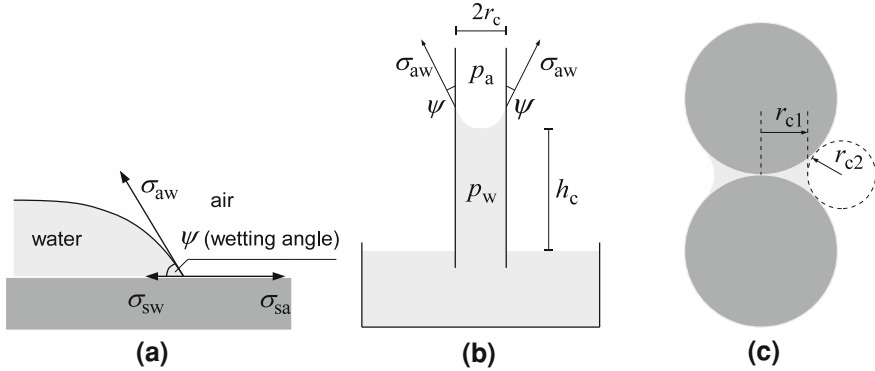
Fig. 2.1 Surface tension effects: **a** equilibrium position of the fluid–fluid interface near the solid surface, **b** rise of the wetting fluid in a capillary tube, **c** pendular ring around the contact point of two solid grains

a perfectly non-wetting fluid, $\psi = 180°$, which results in the formation of spherical droplets on the solid surface.

The existence of surface tension is at the origin of the capillary rise observed in small tubes, Fig. 2.1b. The molecules of the wetting fluid are attracted by the tube wall, and a meniscus (curved interface) forms between water and air above the free surface of water in the recipient. The pressure drop across the interface is denoted in this context as the capillary pressure and can be calculated for a cylindrical tube as:

$$\Delta p = p_c = p_a - p_w = \frac{2\,\sigma_{aw}\,\cos\psi}{r_c} \,, \qquad (2.3)$$

where r_c is the tube radius. Assuming that the value of the surface tension between air and water corresponds to the temperature of 20 °C, the tube material is perfectly wettable ($\psi = 0°$), air is at constant atmospheric pressure everywhere, and water is incompressible, one obtains the well known formula for the height of the capillary rise:

$$h_c = \frac{1.5 \times 10^{-5}}{r_c} \,, \qquad (2.4)$$

where both h_c and r_c are in meters. Equation (2.4) is often used to approximate the height of capillary rise in natural porous media, which are characterized by small wettability angles. However, as the geometry of pores in natural porous media is much more complex, the representation of pore system as a bundle of capillary tubes does not hold in many situations, and more complex configurations of air and water in the pore space are encountered, which will be discussed on the example of a granular porous medium.

Since water molecules are preferentially attracted to the surface of the solid phase, they can be adsorbed from the vapour present in the pore air. Thus, small amounts
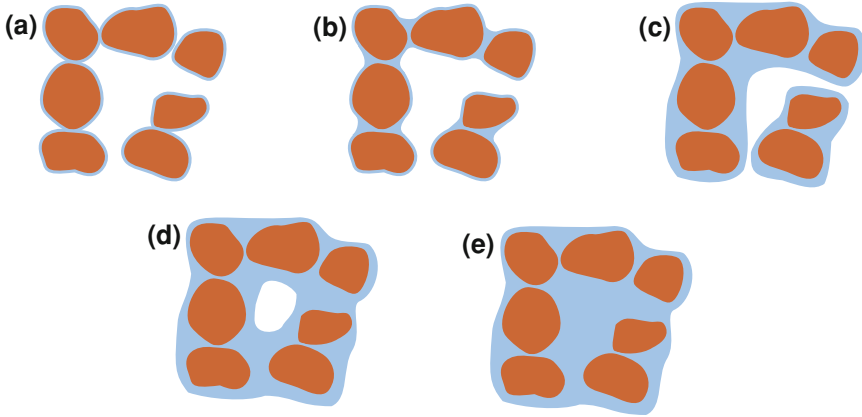
Fig. 2.2 Spatial configurations of water and air in an unsaturated granular porous medium: **a** adsorbed regime, **b** capillary pendular regime, **c** capillary funicular regime, **d** occluded air bubble regime, **e** fully saturated regime

of water are always present in the form of thin films covering the surface of the solid skeleton, Fig. 2.2a. The thickness of this layer depends on the strength of molecular level interactions between solid and water and on the relative air humidity. Due to the tight bonding of the adsorbed water to the solid surface, in many practical problems it is considered as immobile [62]. As the amount of water in a porous medium increases, it is attracted to the water adsorbed at the solid surface by the cohesion forces, but on the other hand tends to minimize the area of the water–air interface. This form of water is known as the capillary water, and occurs initially in acute corners of the pores. If the porous skeleton is made of grains, water forms pendular rings around the contact points, Figs. 2.1c and 2.2b. The corresponding water–air configuration is known as the pendular stage. Pendular water is less tightly bound by the solid phase, but it occurs in isolated regions, and does not form continuous flowpaths, so it can be considered as macroscopically immobile [62]. The pressure drop at the interface between pendular water and pore air can be theoretically calculated from Eq. (2.1), assuming a negative value for r_{c1} and a positive value for r_{c2} (Fig. 2.1c). If more water is added to the system, the regions occupied by pendular water coalesce and continuous thicker films are formed along the pore walls. At this stage, known as the funicular stage, the flow of liquid water is possible, Fig. 2.2c. For all three water configurations mentioned above, air occupies continuously the central part of the pores. As the amount of water in the system increases further, the water films become thicker and pores can be entirely filled with water at the points where their cross-section is smaller. The air phase loses its continuity and no macroscopic air flow is possible. This is called the occluded air bubbles stage. With time the air can dissolve in water and full water saturation is reached. Since in this work evaporation and dissolution are neglected, the considerations presented in the following chapters are applicable to funicular, occluded air, and fully water saturated stages.

Fig. 2.3 Pore-scale representative elementary volume
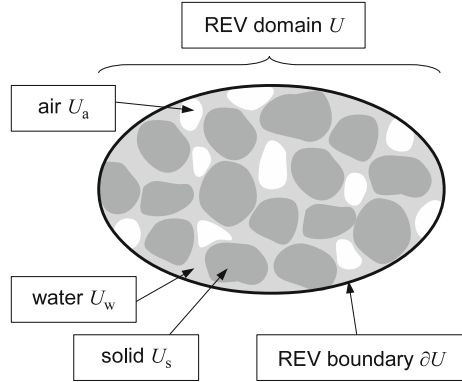
2.1.2 Volume Fractions and Saturations

Continuum description of a multiphase porous medium at the Darcy scale implies that the relevant physical quantities defined at a given point $\mathbf{x}$ represent averages taken over a pore-scale representative elementary volume (REV) associated with that point, Fig. 2.3. At the Darcy scale the same point can be occupied simultaneously by all three phases, which is represented by the concepts of volume fractions and saturations. The volume fraction of phase α is defined as the ratio of the volume of the part of the REV occupied by phase α to the total volume of the REV:

$$\theta_\alpha = \frac{|U_\alpha|}{|U|} .$$
(2.5)

Porosity is defined as the volume fraction of pores, and it is equal to the sum of the volume fractions of the two pore fluids:

$$\phi = \frac{|U_w| + |U_a|}{|U|} = \theta_a + \theta_w .$$
(2.6)

Moreover, it is convenient to define the saturation of each phase, which is equal to the fraction of the pore space occupied by a given fluid:

$$S_\alpha = \frac{\theta_\alpha}{\phi} .$$
(2.7)

The sum of the air and water saturations must be equal to one:

$$S_a + S_w = 1 .$$
(2.8)

In general, each saturation can vary from 0 to 1. However, in most practical problems the range of variability is smaller. For instance, if a fully water-saturated medium is drained, at some point the mobile water (not adsorbed to the solid phase) looses its continuity and the liquid flow will not be possible (transition from the funicular to pendular state). The corresponding value of the water saturation is called residual or irreducible values, and denoted by S_{rw}, respectively. However, it should be noted that the value of water saturation can be further decreased by natural evaporation or oven drying. Similarly, during imbibition in a dry medium in natural conditions, it is generally not possible to achieve full water saturation, as a part of the pores will be occupied by isolated air bubbles. The corresponding residual air saturation is denoted as S_{ra}, respectively. However, the water saturation can increase above the value of $1 - S_{ra}$, for example if the air is compressed or dissolves in water. Therefore, the residual saturations must be considered as problem-specific parameters, not material parameters [31].

For practical purposes, the fluid saturations are often normalized with respect to the range of values occurring in the problem under consideration. The resulting normalized (effective) saturations are defined as:

$$S_{e\alpha} = \frac{S_\alpha - S_\alpha^{min}}{S_\alpha^{max} - S_\alpha^{min}} \,, \tag{2.9}$$

where S_α^{max} and S_α^{min} are the maximum and minimum saturation values occurring for a given problem.

In soil physics and hydrology it is more common to quantify the relative amount of fluid phases in soil using the volumetric fractions θ_α. If the compressibility of the solid skeleton is neglected ($\phi = const$), the volumetric phase contents are uniquely defined by phase saturations. In field conditions the volumetric fraction of water varies between the residual water content:

$$\theta_{rw} = \phi \, S_{rw} \,, \tag{2.10}$$

and the so-called saturated water content:

$$\theta_{sw} = \phi \, (1 - S_{ra}) \,. \tag{2.11}$$

The latter value refers to the state of maximum attainable water saturation. Equivalent limit values can be defined also for the volumetric air content.

2.1.3 Fluid Potentials

At the Darcy scale, the energy state of each of the two fluids present in the pore space is commonly characterized using the concept of energy potential. The energy

potential is related to the forces acting on the fluid. It is defined as the negative integral of the force over the path taken by an infinitesimally small volume of water, when it moves from a reference location to the point under consideration [58]. The reference point is commonly assumed to be at the surface of a free water body located at the same elevation as the considered volume of the pore fluid, and subjected to normal atmospheric pressure. Thus, the values of the fluid potentials are relative to the normal atmospheric pressure. Potentials can be expressed as energy per unit mass ($J\,kg^{-1}$), energy per unit volume ($Jm^{-3} = Pa$) or energy per unit weight ($Jkg^{-1}m^{-1}s^2 = m$).

Assuming that the fluid density depends only on its pressure and that the only mass force is the gravity, acting in the direction of decreasing elevation z, the potential of each pore fluid can be conveniently expressed in terms of the total hydraulic head:

$$H_\alpha = \int_{p_\alpha^{\text{ref}}}^{p_\alpha} \frac{d\hat{p}}{\rho_\alpha(\hat{p})g} + z = h_\alpha + z, \qquad (2.12)$$

where p_α^{ref} is the reference pressure, ρ_α is the fluid density, $\hat{p}$ is the integration variable, g is the magnitude of gravitational acceleration, z is the elevation above the reference level, and h_α is the pressure head. As far as the water phase is considered, in the fully water-saturated conditions the variable p_w represents the pressure exerted by unsupported water phase overlying the point of interest, while in partially saturated conditions it accounts for the effect of capillary and adsorption forces binding water molecules to the solid skeleton. These interactions include short range van der Waals forces between water and solid, cohesion through hydrogen bonds in water and ion hydration and binding of water in diffuse double layers [48, 58]. In the case of the air phase (or the non-wetting fluid in general) the variable p_a represents only the pressure, as the interaction between this phase and the solid skeleton is typically neglected.

The difference between the pressure potentials of air and water in unsaturated conditions, caused by the action of capillary and adsorption forces, is often called the capillary pressure, by analogy to the pore-scale capillary pressure defined by Eq. (2.3). The capillary pressure at the Darcy scale is assumed to be a function of the water saturation:

$$p_a - p_w = p_c(S_w) . \qquad (2.13)$$

In hydrophilic porous media the capillary pressure is always nonnegative. If the pore air pressure is constant, p_c increases with decreasing water saturation, while the water pressure potential decreases correspondingly. This is caused by the fact that as the water saturation decreases, the relative amount of water molecules bound by strong short range forces to the solid surface increases.

There are important differences between the pore-scale and Darcy-scale capillary pressure. According to Eq. (2.3), the pressure is larger in the fluid occupying the concave side of the interface. Therefore, from the pore scale point of view, the water pressure is lower than the air pressure in pendular rings or in capillary tubes, but it is higher

than the air pressure in the thin water layers around spherical solid grains, or around occluded air bubbles. However, in each of these situations the Darcy-scale capillary pressure is defined as a nonnegative value. Due to this discrepancy, some authors prefer to use the term suction potential, instead of the capillary potential, and the term matric potential, instead of the water pressure in the unsaturated zone, e.g. [58]. Indeed, the values of the water pressure potential at low saturations, measured with respect to the atmospheric pressure, are often well below -100 kPa, which would indicate negative absolute pressures. In this work, the terms capillary pressure and water pressure are used, with a full recognition of the fact that in unsaturated conditions they refer to the average energy state of water within a representative elementary volume, rather than the physical pressure in the liquid water.

2.1.4 Capillary Function

The relationship between Darcy-scale capillary pressure and water saturation is known under a number of names, such as the capillary function, suction function, retention function, or soil water characteristic function [41, 48, 58, 63]. Figure 2.4 presents its basic features, in relation to various configurations of air and water in a porous medium. Usually, if the medium is fully water-saturated, it can be invaded by the air phase only if the air pressure exceeds the water pressure by a specific value. The corresponding value of p_c is called air-entry pressure or bubbling pressure [41, 58]. This effect can be explained if the medium is conceptualized as a bundle of capillary tubes. According to the Laplace law, Eq. (2.3), all tubes remain saturated, if the water pressure is lower than the pressure of the surrounding air, but the capillary pressure ($p_a - p_w$) does not exceed the maximum possible value for the largest tube. After this value has been exceeded, the largest tube drains and the overall saturation of the system becomes smaller than one. In natural porous media the value of the air entry pressure corresponds to the diameter of the largest pore forming a connected path through the system. The air entry pressure is more often observed in granular media with relatively uniform grain size, and may be not pronounced in fine-textured media [41]. Above the value of the air entry pressure, the water saturation decreases with the increasing value of the capillary potential. The slope of the curve is determined by the uniformity of the size of pores. If the pores have very similar size, most of them drain quickly above the entry pressure and the slope of the curve is very steep. If the pores show large variability in size, at each increment of the potential only a small part of the pores will be drained, and the decrease in saturation is much more gradual. At some point, the value of the residual water saturation is reached, and further liquid flow is inhibited by the lack of connectivity of the pendular capillary water. The saturation can be further decreased by evaporation, but this requires very large increments of the potential. The capillary pressure can be related to the air relative humidity by the Kelvin equation [58]:
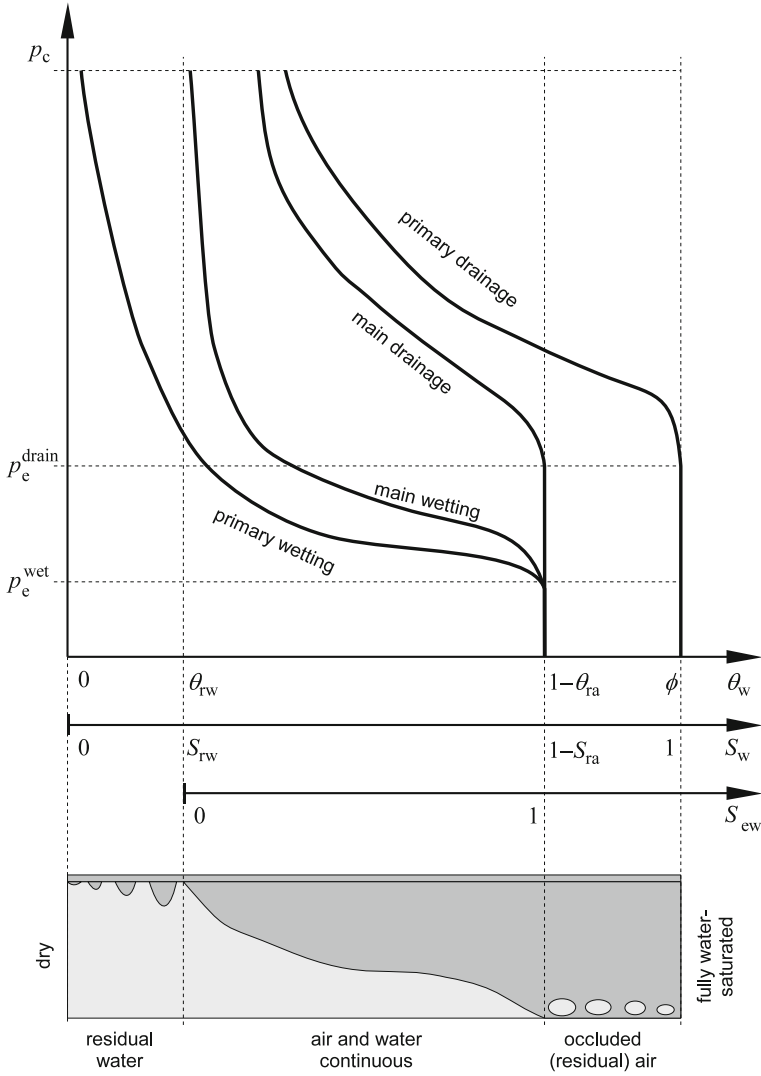
Fig. 2.4 Capillary pressure–water saturation relationship for various air and water flow regimes

$$p_c = -\frac{R_{gas}\,\mathscr{T}\,\rho_w}{\mathscr{M}_w}\ln(\mathscr{H})\ ,\tag{2.14}$$

where R_{gas} is the universal gas constant $\left(R_{gas} = 8.31\,\mathrm{J\,mol^{-1}\,K^{-1}}\right)$, $\mathscr{T}$ is the Kelvin temperature, $\mathscr{M}_w$ is the mole mass of water $\left(\mathscr{M}_w = 0.018\,\mathrm{kg\,mol^{-1}}\right)$, and $\mathscr{H}$ is the relative air humidity. For oven dry conditions the potential value of about $10^6\,\mathrm{kPa}$ is

reported in the literature, which corresponds to the relative air humidity of 0.01 % [21, 45].

It is important to note that the capillary pressure–saturation relationship shows hysteresis and depends on the history of the flow. The drying process described above corresponds to the so-called primary drainage curve. A complementary relationship, i.e. the primary imbition curve, can be obtained by increasing the water saturation, starting from oven-dry conditions. During imbition the values of the capillary potential corresponding to a given water saturation are smaller than during the primary drainage. Moreover, it is in general not possible to reach full water saturation during imbition, due to the trapping of air bubbles. The maximum possible water saturation $1 - S_{ra}$ can be achieved for a value of the capillary potential larger than zero. This value is the counterpart of the air-entry pressure at the primary drainage curve, and is sometimes called the water-entry pressure [41]. As the latter term has also other meanings, in this work the term air-entry pressure, or simply entry pressure is consistently used for the characteristic value of the capillary pressure above which air flow is possible, in relation to both imbition and drainage. The entry pressure at the imbition curve is smaller than at the drainage curve, and sometimes does not appear at all, i.e. the maximum saturation is reached only at $p_c = 0$. In many practical problems the water saturation varies between the residual value S_{rw} and the maximum value $1 - S_{ra}$. The drainage process from $1 - S_{ra}$ to S_{rw} is described by the main drainage curve, while the corresponding imbition process by the main imbition (or wetting) curve. If the flow direction is reversed before the limit saturation is reached, the capillary pressure and saturation follow a so-called scanning curve, which is a path in the area enclosed by the main curves.

The hysteresis is usually explained by the variations in the value of the wetting angle between advancing and receding fluid at the solid surface, by the pore-scale trapping of air and by the ink-bottle effect, e.g. [41, 63]. The latter one is related to the fact that during imbition the possibility of capillary flow is controlled by the widest cross-section of the pore, while during drainage it is controlled by the smallest cross-section. In this work the hysteresis of the capillary function at the Darcy scale is not considered. However, in Chap. 7 it will be shown that a quasi-hysteresis may occur in the field-scale capillary function for a porous medium that shows a specific heterogeneous structure at the Darcy scale.

For practical purposes it is convenient to express the capillary function, for either imbition or drainage, as an analytical function. A large number of such analytical formulae can be found in the literature. In this section only the ones used in the following part of this book are presented. For a more detailed reviews of various propositions, see [38, 43, 45]. Typically, the formulae are expressed in terms of the normalized water saturation, Eq. (2.9). The choice of the parameters S_w^{min} and S_w^{max} depends on the problem under consideration. For the primary drainage with subsequent drying $S_w^{max} = 1$ and $S_w^{min} = 0$, for the primary imbition $S_w^{max} = 1 - S_{ra}$ and $S_w^{min} = 0$, while for the main drainage and imbition curves $S_w^{max} = 1 - S_{ra}$ and $S_w^{min} = S_{rw}$.

For the sake of consistency all the following functions have the capillary pressure p_c as their argument. In fact some of them were originally written in terms of the

capillary pressure head h_c. Transition to the pressure head based form is straightforward and requires only that the parameters p_e and p_g are replaced by the corresponding pressure heads.

One of the most often used analytical models, proposed by Brooks and Corey [7], can be written in the following form:

$$S_{ew} = \begin{cases} (p_c/p_e)^{-n_b} & \text{if} \quad p_c > p_e \\ 1 & \text{if} \quad p_c \leq p_e \end{cases} , \tag{2.15}$$

$$p_c = p_e \ (S_{ew})^{-1/n_b} , \tag{2.16}$$

where p_e is the air-entry pressure and n_b is a parameter related to the pore-size distribution, generally ranging from 0.2 to 5. Large values of n_b correspond to a rapid decrease of the saturation above the entry pressure, which is typical for media having uniformly sized pores. Smaller values of n_b characterize media with non-uniform pore size distributions. This model is useful for porous media having a distinct air entry pressure and relatively uniform pore sizes, however it cannot reproduce the inflection point in the capillary function, characteristic for many finely textured soils [41].

Another well-known model, introduced by van Genuchten [79], has the following form:

$$S_{ew} = \left[1 + (p_c/p_g)^{n_g}\right]^{-m_g} , \tag{2.17}$$

$$p_c = p_g \left[(S_{ew})^{-1/m_g} - 1\right]^{1/n_g} , \tag{2.18}$$

where p_g is a pressure scaling parameter, related to the average size of the pores (in the original paper its inverse $\alpha_g = 1/p_g$ was used). The value of p_g approximately corresponds to the position of the inflection point at the capillary curve described by Eq. (2.17). The exponents m_g and n_g are related to the pore size distribution, and in principle can be considered as independent of each other. However, in order to reduce the number of independent parameters, and to develop analytical formulae for the relative permeability (discussed later in Sect. 2.1.6), it is often assumed that $m_g = 1 - 1/n_g$ or $m_g = 1 - 2/n_g$. The van Genuchten function does not account explicitly for the air-entry pressure, although for some values of n_g and m_g saturations very close to unity can be obtained for a certain range of the capillary pressures above zero. Some authors proposed to introduce the air-entry pressure as an additional explicit parameter in the van Genuchten model [34, 81]. In the special case of $m_g = 1$ the van Genuchten function reduces to the Gardner function [23]:

$$S_{ew} = \frac{1}{1 + (p_c/p_g)^{n_g}} , \tag{2.19}$$

$$p_c = p_g (S_{ew} - 1)^{1/n_g} . \tag{2.20}$$

Table 2.1 Parameters of the van Genuchten ($m_g = 1 - 1/n_g$) and Brooks–Corey capillary functions for various types of soil (van Genuchten function parameters from [10])

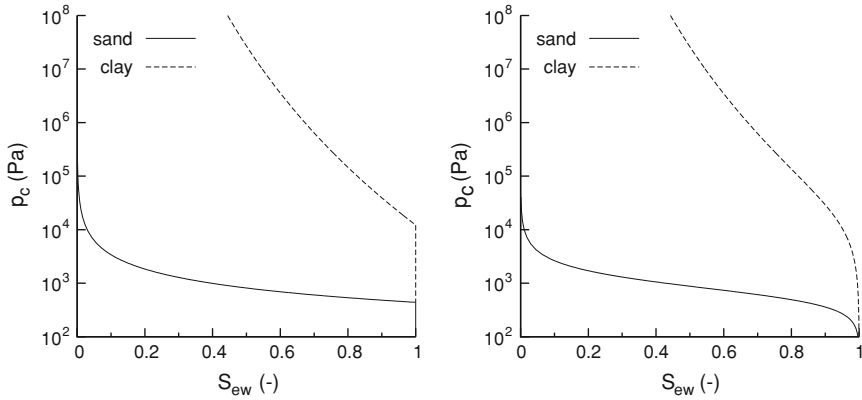|	p_g (Pa)	n_g (–)	p_e (Pa)	n_b (–)	θ_{sw} (–)	θ_{rw} (–)	K_{sw} (m s^{-1})
sand	677	2.68	440	1.124	0.43	0.045	8.25E−5
loamy sand	791	2.28	498	0.908	0.41	0.057	4.05E−5
sandy loam	1308	1.89	814	0.908	0.41	0.065	1.23E−5
loam	2725	1.56	1779	0.719	0.43	0.078	2.89E−6
silt	6131	1.37	4462	0.710	0.46	0.034	6.94E−7
clay	12263	1.09	12203	0.090	0.38	0.068	5.56E−7

Fig. 2.5 Typical capillary functions for sand and clay

Lenhard et al. [44] established analytical relationships between the parameters of Brooks–Corey function and van Genuchten function (with $m_g = 1 - 1/n_g$) for the same porous material, based on the slope of the curves at normalized saturation equal to 0.5. They are given by the following formulae:

$$n_b = (n_g - 1)\left(1 - 0.5^{n_g/(n_g-1)}\right), \tag{2.21}$$

$$Z_s = 0.72 - 0.35 \exp\left(-(n_g)^4\right), \tag{2.22}$$

$$p_e = p_g \left(Z_s\right)^{1/n_b} \left[(Z_s)^{n_g/(1-n_g)} - 1\right]^{1/n_g}, \tag{2.23}$$

where Z_s is an auxiliary parameter. Typical values of the parameters of the van Genuchten and Brooks–Corey models for several types of soil are listed in Table 2.1. The van Genuchten function parameters were taken from [10]. The corresponding Brooks–Corey function parameters were calculated using the above formulae. Figure 2.5 shows the capillary functions for sand and clay, according to both models.

A relatively simple exponential formula is often used in the development of analytical solutions for the Richards equation, e.g. [3, 68]:

$$S_{ew} = \begin{cases} \exp\left(-\dfrac{p_c - p_e}{p_g}\right) & \text{if} \quad p_c > p_e \\ 1 & \text{if} \quad p_c \le p_e \end{cases} , \qquad (2.24)$$

$$p_c = p_e - p_g \, \ln(S_{ew}) , \qquad (2.25)$$

where p_e is the air entry pressure and p_g is a pressure scaling parameter. This formula can be considered as a complementary relationship to the Gardner exponential relative permeability function (introduced later in Sect. 2.1.6).

Note that all the above formulae predict infinite value of the capillary pressure as the normalized saturation approaches zero, which is not consistent with the fact mentioned earlier, that even for oven-dry conditions the capillary pressure has a finite value of about 10^6 kPa. Therefore, Eqs. (2.15)–(2.24) should be considered valid only in the range of normalized water saturations significantly larger than zero. For the dry range the capillary functions should be appropriately modified, to ensure a finite value of the capillary pressure at zero water saturation [21, 37].

2.1.5 Darcy Equation

At the pore scale, the momentum conservation principle for each fluid phase is represented by the Navier-Stokes equations. In the case of steady, laminar flow of incompressible newtonian fluid α in a horizontal tube having a uniform circular cross-section, the Navier-Stokes equations reduce to the Poiseuille equation, which gives the following formula for the average fluid velocity v_α [4]:

$$v_\alpha = -\frac{r_c^2}{8\,\mu_\alpha} \frac{d\,p_\alpha}{d\,x} , \qquad (2.26)$$

where r_c is the tube radius and μ_α is the dynamic viscosity coefficient of the fluid. An important feature of this relationship is that the average velocity is directly proportional to the pressure gradient, and the proportionality coefficient depends on the geometric parameters and the fluid viscosity. In a more general case of three-dimensional single-phase fluid flow in a medium characterized by arbitrary pore geometry, a mathematically rigorous averaging of the pore scale Navier-Stokes equations yields the following result, e.g. [2, 4, 28, 86]:

$$\mathbf{v}_\alpha = -\frac{k_s}{\mu_\alpha} (\nabla p_\alpha - \rho_\alpha \, \mathbf{g}) , \qquad (2.27)$$

where $\mathsf{k_s}$ is the absolute (or intrinsic) permeability tensor and $\mathbf{g}$ is the gravity vector. Intrinsic permeability has dimension of m^2 and depends only on the geometric characteristics of the pores. Its value can be computed for a given geometry of pores, by solving Stokes equations in a representative elementary volume [77]. Alternatively, it can be estimated using many empirical or semi-empirical formulae, developed particularly for granular media, for instance those proposed by Hazen or Kozeny and Carman [39, 82]. For practical purposes, however, the most reliable estimation of permeability is obtained from laboratory or field measurements. Equation (2.27) was derived from the pore-scale flow equations by several authors, e.g. [4, 28, 86]. The most important assumptions introduced in the derivation of Eq. (2.27) can be summarized as follows [31]:

- Inertial effects are neglected, i.e. quasi-steady fluid flow is assumed.
- The flow is laminar.
- The viscous part of the stress tensor in fluid behaves according to the Newton law.

Equation (2.27) can be rewritten it terms of the hydraulic head as:

$$\mathbf{v}_\alpha = -\frac{\mathsf{k_s}\,\rho_\alpha\,g}{\mu_\alpha}\,\nabla H_\alpha = -\mathsf{K}_{\mathsf{s}\alpha}\,\nabla H_\alpha\ , \tag{2.28}$$

where $\mathsf{K}_{\mathsf{s}\alpha}$ is the hydraulic conductivity tensor for single-phase flow, which depends on the properties of porous medium and the pore fluid. Equations (2.27) and (2.28) represent an extension to three dimensions of the linear flow law, which was established experimentally for the one-dimensional case by Darcy [14]. The head-based form of the Darcy formula is often used in groundwater flow simulations, when the variations of fluid density and viscosity are negligible, and the hydraulic conductivity with respect to water K_{sw} can be considered constant.

If two fluids flow within the pore space, it is often assumed that their velocities can be expressed by the following extended form of the Darcy formula, e.g. [63]:

$$\mathbf{v}_\alpha = -\frac{\mathsf{k}_\alpha\,(S_\alpha)}{\mu_\alpha}\,(\nabla p_\alpha - \rho_\alpha\,\mathbf{g}) = -\mathsf{K}_\alpha\,(S_\alpha)\,\nabla H_\alpha\ , \tag{2.29}$$

where k_α and K_α are permeability and conductivity tensors, which depend on the saturation of phase α. In a general case of anisotropic porous medium, the relationship between permeability and saturation will be different for each component of the permeability tensor. However, for practical purposes a simplified relationship is often postulated in the following form:

$$\mathsf{k}_\alpha\,(S_\alpha) = \mathsf{k_s}\,k_{\mathrm{r}\alpha}\,(S_\alpha)\ , \tag{2.30}$$

where $k_{\mathrm{r}\alpha}$ is a scalar relative permeability coefficient, assuming values from zero to one. The equivalent relationship for the hydraulic conductivity tensor is:

$$\mathsf{K}_\alpha\,(S_\alpha) = \mathsf{K}_{\mathsf{s}\alpha}\,k_{\mathrm{r}\alpha}\,(S_\alpha)\ , \tag{2.31}$$

The maximum value $k_{r\alpha} = 1$ corresponds to the case of full saturation with fluid phase α. The minimum value $k_{r\alpha} = 0$ occurs when the fluid phase becomes immobilized, which corresponds to the fluid saturations below the residual saturation $S_\alpha \leq S_{r\alpha}$. Alternatively, the extended Darcy formula can be rewritten in the following form:

$$\mathbf{v}_\alpha = -\mathsf{k}_s\, \lambda_\alpha\, (S_\alpha)\, (\nabla p_\alpha - \rho_\alpha\, \mathbf{g}) \ , \tag{2.32}$$

where $\lambda_\alpha\, (S_\alpha) = k_{r\alpha}\, (S_\alpha)\, /\mu_\alpha$ is the phase mobility.

In contrast to Eq. (2.27), the extension of Darcy equation for multiphase flow given by Eq. (2.29) should be considered as purely phenomenological. As shown by several authors, e.g. [1, 29], in the case of two fluid phases a rigorous averaging of pore-scale momentum conservation leads to coupled Darcy-scale equations, where the flow velocity of each phase depends on the potential gradients in both fluid phases. Such results are consistent with the Onsager reciprocity theorem [66]. These limitations notwithstanding, in the present work Eq. (2.29) is assumed to be a valid approximation of two-phase flow in porous media at the Darcy scale.

2.1.6 Relative Permeability Functions

Since the relative permeability of fluid phase α varies from $k_{r\alpha} = 0$ for $S_\alpha = S_{r\alpha}$ to $k_{r\alpha} = 1$ for $S_\alpha = 1$, it can be conveniently represented by a function of the normalized saturation of each phase, as given by Eq. (2.9), assuming $S_\alpha^{min} = S_{r\alpha}$ and $S_\alpha^{max} = 1$. However, in order to simplify the model formulation, the capillary function and permeability functions for both fluids are typically defined with respect to the water saturation normalized in the range between $S_w^{min} = S_{rw}$ and $S_w^{max} = 1 - S_{ra}$. In such a case, the relative permeability equals unity for the actual fluid saturation smaller than one. In order to keep the physical consistency of the model, k_s is interpreted as the maximum permeability attainable for the considered problem, which can be different for each phase, and is generally smaller than the permeability tensor for single phase flow. In soil hydrology and soil physics the maximum attainable value of the water conductivity:

$$\mathsf{K}_{sw} = \mathsf{k}_s\, \frac{\rho_w\, g}{\mu_w} \ , \tag{2.33}$$

is often referred to as the saturated hydraulic conductivity. However, it corresponds to the state of apparent saturation, with the corresponding volumetric water content θ_{sw} smaller than the porosity ϕ. The formulae for relative permeability presented below can be used in conjunction with various definitions of the normalized water saturation S_{ew}.

Simple power-type relationships between the normalized saturation and the relative permeabilities are often postulated, e.g. [42, 63]:

$$k_{rw} = (S_{ew})^{\eta_w} \ , \tag{2.34}$$

$$k_{ra} = (1 - S_{ew})^{\eta_a} \ , \tag{2.35}$$

Table 2.2 Parameters used in Burdine and Mualem relative permeability models

	κ	η_1	η_2	η_3	η_4
Mualem	0.5	1.0	2.0	$2.5 + 2.0/n_{bc}$	$1.0 + 1.0/n_{bc}$
Burdine	2.0	2.0	1.0	$3.0 + 2.0/n_{bc}$	$1.0 + 2.0/n_{bc}$

where the exponents η_w and η_a are fitting parameters. Relationships of this type can be obtained on the theoretical basis, for simple models of laminar flow in bundles of capillary tubes [54]. As it is the wetting fluid, water tends to move along the solid phase surface and preferentially fills smaller pores. Therefore, at the same saturation of each fluid the resistance of the medium to the flow of water is larger than the resistance to the flow of air. Thus, the exponent η_w is typically larger than η_a.

More sophisticated models of the relative permeability are based on the consideration of statistical distribution of the pore size within the medium, and the connectivity between pores of various sizes. The pore size distribution can be computed from the capillary function, due to the inverse relationship between the capillary radius and the capillary pressure, as given by the Laplace law, Eq. (2.3). The connectivity parameter is more difficult to derive theoretically and is often used as a fitting parameter in the resulting model. Two well known statistical models were proposed by Burdine [9] and Mualem [53]. They can be written in the following generalized form:

$$k_{rw}\left(S_{ew}\right) = \left(S_{ew}\right)^{\kappa} \left[\frac{\int_0^{S_{ew}} p_c(\hat{S})^{-\eta_1} \, d\hat{S}}{\int_0^1 p_c(\hat{S})^{-\eta_1} \, d\hat{S}} \right]^{\eta_2}, \tag{2.36}$$

$$k_{ra}\left(S_{ew}\right) = \left(1 - S_{ew}\right)^{\kappa} \left[\frac{\int_{S_{ew}}^1 p_c(\hat{S})^{-\eta_1} \, d\hat{S}}{\int_0^1 p_c(\hat{S})^{-\eta_1} \, d\hat{S}} \right]^{\eta_2}, \tag{2.37}$$

where $\hat{S}$ denotes the integration variable and the values of the connectivity parameter κ and the exponents η_1 and η_2 are listed in Table 2.2.

In a general case the application of these models to an arbitrary $p_c(S_{ew})$ function requires numerical integration. In some cases, however, the integrals can be evaluated analytically. In particular, it is possible for the Brooks–Corey capillary function, for which the following formulae are obtained:

$$k_{rw}\left(S_{ew}\right) = \left(S_{ew}\right)^{\eta_3}, \tag{2.38}$$

$$k_{rw}\left(S_{ew}\right) = \left(1 - S_{ew}\right)^{\kappa} \left[1 - \left(S_{ew}\right)^{\eta_4}\right]^{\eta_2}, \tag{2.39}$$

where the exponents η_3 and η_4 are given in Table 2.2. Note that the relative permeability of the water phase is given by a simple power law, similarly as in Eq. (2.34). In the case of van Genuchten capillary function, the Mualem formula can be integrated analytically if $m_g = 1 - 1/n_g$, leading to the following result:

$$k_{\mathrm{rw}}(S_{\mathrm{ew}}) = S_{\mathrm{ew}}^{\kappa}\left[1 - \left(1 - (S_{\mathrm{ew}})^{1/m_{\mathrm{g}}}\right)^{m_{\mathrm{g}}}\right]^2 , \tag{2.40}$$

$$k_{\mathrm{ra}}(S_{\mathrm{ew}}) = (1 - S_{\mathrm{ew}})^{\kappa}\left[1 - (S_{\mathrm{ew}})^{1/m_{\mathrm{g}}}\right]^{2\,m_{\mathrm{g}}} . \tag{2.41}$$

In general, the connectivity factor κ can be treated as a fitting parameter of the model. Improved agreement with laboratory measurements was reported for negative values ranging from -1.28 for sands to -5.96 for clays [69]. The value of $\kappa = 1/3$ was suggested for the non-wetting phase relative permeability [49].

The Burdine approach provides a closed-form analytical result for the van Genuchten capillary function if $m_{\mathrm{g}} = 1 - 2/n_{\mathrm{g}}$:

$$k_{\mathrm{rw}}(S_{\mathrm{ew}}) = S_{\mathrm{ew}}^{\kappa}\left[1 - \left(1 - (S_{\mathrm{ew}})^{1/m_{\mathrm{g}}}\right)^{m_{\mathrm{g}}}\right] , \tag{2.42}$$

$$k_{\mathrm{ra}}(S_{\mathrm{ew}}) = (1 - S_{\mathrm{ew}})^{\kappa}\left[1 - (S_{\mathrm{ew}})^{1/m_{\mathrm{g}}}\right]^{m_{\mathrm{g}}} . \tag{2.43}$$

All the above formulae can be rearranged using the relevant analytical expressions for $S_{\mathrm{ew}}(p_c)$ functions, in order to express the relative permeability of each phase as a function of the capillary pressure. Typical relative permeability functions for sand and clay according to Brooks–Corey–Burdine and van Genuchten–Mualem models are shown in Fig. 2.6. Parameters of the porous media are taken from Table 2.1. Significant differences between the two models are observed for clay. The van Genuchten–Mualem model predicts a rapid decrease of the relative water permeability and a rapid increase of the relative air permeability as the capillary pressure increases only slightly from 0 to 100 Pa, which is inconsistent with the fact that the water saturation in this range remains virtually constant and very close to 1. The reason for this discrepancy is related to the integrals in formulae (2.36) and (2.37), where, in the absence of the air-entry pressure, the inverse of the capillary pressure tends to infinity as the water saturation tends to one. As a remedy, introduction of the air-entry pressure as an additional parameter in the van Genuchten model is recommended [34, 81].

Some empirical models define the relative permeability directly as a function of the capillary pressure. Such approaches are typically used for the Richards equation, where the assumption of constant air pressure allows to express the relative water permeability as a function of the water pressure only. To this group belongs the widely used exponential formula, originally suggested by Gardner [23] and modified by Philip [61]:

$$k_{\mathrm{rw}}(p_{\mathrm{c}}) = \begin{cases} \exp\left(-\dfrac{p_{\mathrm{c}} - p_{\mathrm{e}}}{p_{\mathrm{g}}}\right) & \text{if } p_c > p_e , \\ 1 & \text{if } p_{\mathrm{c}} \le p_{\mathrm{e}} \end{cases} \tag{2.44}$$

where p_{e} and p_{g} have the same meaning as in Eq. (2.24). Another well-known formula was also proposed by Gardner [23]:
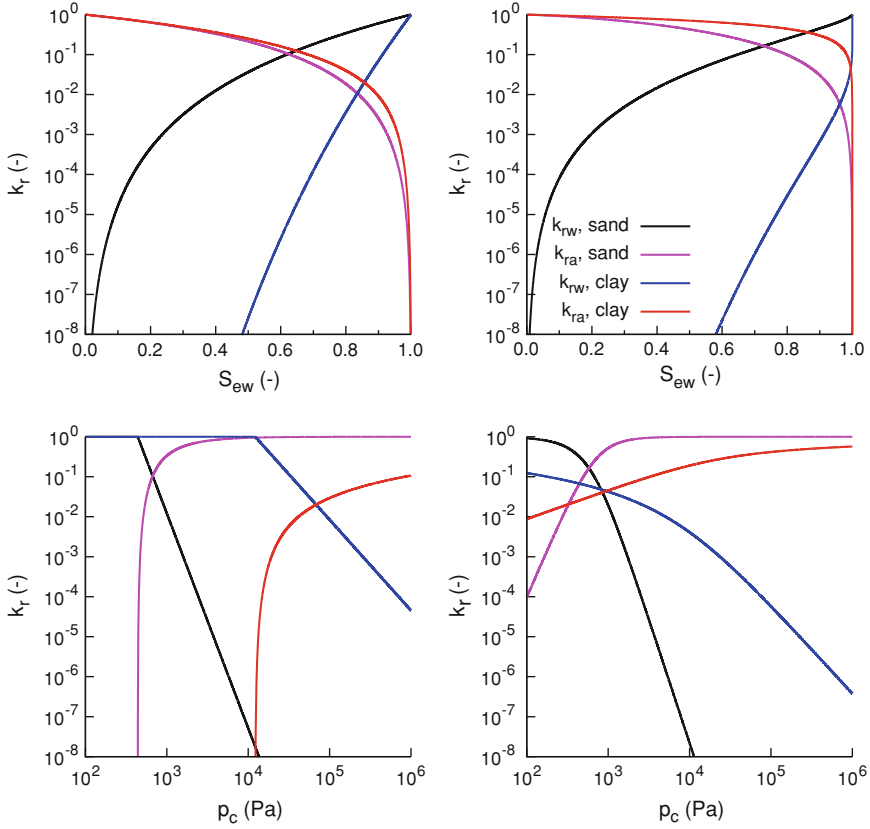
Fig. 2.6 Typical relative permeability functions for sand and clay according to Brooks–Corey–Burdine model (*left*) and van Genuchten–Mualem model (*right*). At the *top* $k_r(S_{ew})$ functions, at the *bottom* $k_r(p_c)$ functions

$$k_{rw}(p_c) = \frac{1}{1 + \left(p_c/p_g\right)^{\eta_w}} \ . \tag{2.45}$$

The above analytical expression has the same form as the formula for the capillary function in Eq. (2.19). Equations (2.44) and (2.45) can be alternatively expressed in terms of the capillary pressure head.

2.1.7 Density and Viscosity of Fluids

In general, the density of the water phase depends on the temperature, pressure and the concentration of dissolved substances. For pure water in isothermal conditions, the dependence of density on the pressure can be expressed as follows [31]:

$$\rho_{\mathrm{w}}(p_{\mathrm{w}}) = \rho_{\mathrm{w}}^{\mathrm{ref}} \, \exp\left[\beta_{\mathrm{w}}\left(p_{\mathrm{w}} - p_{\mathrm{w}}^{\mathrm{ref}}\right)\right] , \qquad (2.46)$$

where $\rho_{\mathrm{w}}^{\mathrm{ref}}$ is the reference water density ($1000\,\mathrm{kg\,m^{-3}}$ at $20\,°\mathrm{C}$), $p_{\mathrm{w}}^{\mathrm{ref}}$ is the standard atmospheric pressure ($101325\,\mathrm{Pa}$) and β_{w} is the isothermal relative compressibility coefficient. For the range of temperatures from 10 to $50\,°\mathrm{C}$ and pressures from 0 to $10^6\,\mathrm{Pa}$, β_{w} is approximately constant and equal to $4.5 \times 10^{-10}\,\mathrm{Pa^{-1}}$. This value of β_{w} corresponds to a change of density of approximately $0.5\,\mathrm{kg\,m^{-3}}$, if the pressure changes by $10^6\,\mathrm{Pa}$.

While in many practical applications water is considered incompressible, its compressibility is included in this work, in order to keep consistency in the presentation of the governing equations for both fluid phases, and in order to maintain parabolic character of the governing equation for the water flow in fully saturated rigid porous medium. Application of the above formula is questionable for unsaturated conditions, where p_{w} is a measure of the energy potential rather than the actual pressure of the water phase and assumes very large negative values [25]. In the examples considered in this work the values of p_{w} do not fall below $-10^6\,\mathrm{Pa}$, and the discrepancy is neglected. Similarly to the density, the viscosity of water depends on the temperature, pressure and chemical composition. For the purposes of the present analysis, these dependencies are neglected, and a constant value of water viscosity is assumed $\mu_w = 10^{-3}\,\mathrm{Pa\,s}$, which corresponds to the temperature of $20\,°\mathrm{C}$.

The density of dry air can be obtained from the ideal gas law [31]:

$$\rho_{\mathrm{a}} = \frac{\mathscr{M}_{\mathrm{a}}\, p_{\mathrm{a}}}{R_{\mathrm{gas}}\, \mathscr{T}} = c_{\mathrm{a}}\, p_{\mathrm{a}} , \qquad (2.47)$$

where p_{a} is the air pressure, $\mathscr{M}_{\mathrm{a}}$ is the molecular mass of air ($0.0029\,\mathrm{kg\,mol^{-1}}$), R_{gas} is the universal gas constant ($8.314\,\mathrm{J\,mol^{-1}\,K^{-1}}$), $\mathscr{T}$ is temperature in degrees Kelvin and c_{a} is the absolute compressibility coefficient for air. In the temperature of $20\,°\mathrm{C} = 293.16\,°\mathrm{K}$ and at the normal atmospheric pressure the density of dry air is $\rho_{\mathrm{a}} = 1.206\,\mathrm{kg\,m^{-3}}$. The density of pore air varies according to the changes in the content of water vapour, but this effects are neglected in the present work. The viscosity of air is assumed constant and equal to $\mu_{\mathrm{a}} = 1.83 \times 10^{-5}\,\mathrm{Pa\,s}$.

2.2 Governing Equations for Fluid Flow

2.2.1 Two-Phase Flow

The governing equations for two-phase flow in a porous medium are derived from the mass conservation principle, applied to a Darcy-scale representative elementary volume, as shown in Fig. 2.3. In the absence of source/sink terms, the change in the total mass of fluid phase α inside the REV must be balanced by the total mass flux across the REV boundary. For a rigid solid phase this can be written as:

$$\frac{\partial}{\partial t} \int_U \rho_\alpha \, S_\alpha \, \phi \, \mathrm{d}U = \int_{\partial U} \rho_\alpha \, \mathbf{v}_\alpha \, \mathbf{n}_U \, \mathrm{d}\partial U \,, \tag{2.48}$$

where ∂U is the boundary of the REV and $\mathbf{n}_U$ is a unit vector normal to ∂U and directed outwards. Using the Gauss-Ostrogradski theorem and assuming immovable REV boundaries, Eq. (2.48) can be transformed to a differential (strong) form:

$$\frac{\partial}{\partial t} (\rho_\alpha \, S_\alpha \, \phi) + \nabla \, (\rho_\alpha \, \mathbf{v}_\alpha) = 0 \,. \tag{2.49}$$

The velocity of each fluid phase with respect to the solid phase is given by the extended Darcy formula, Eq. (2.29). Substitution of the Darcy equation into the mass balance equation for each phase results in the following system of two coupled partial differential equations:

$$\frac{\partial}{\partial t} (\rho_\mathrm{w} \, S_\mathrm{w} \, \phi) - \nabla \left[\frac{\rho_\mathrm{w} \, k_\mathrm{s} \, k_\mathrm{rw}}{\mu_\mathrm{w}} \, (\nabla \, p_\mathrm{w} - \rho_\mathrm{w} \, \mathbf{g}) \right] = 0 \,, \tag{2.50}$$

$$\frac{\partial}{\partial t} (\rho_\mathrm{a} \, S_\mathrm{a} \, \phi) - \nabla \left[\frac{\rho_\mathrm{a} \, k_\mathrm{s} \, k_\mathrm{ra}}{\mu_\mathrm{a}} \, (\nabla \, p_\mathrm{a} - \rho_\mathrm{a} \, \mathbf{g}) \right] = 0 \,. \tag{2.51}$$

Using the chain differentiation rule the storage term for each phase can be expanded to show explicitly the contributions related to the fluid compressibility and saturation change:

$$\begin{aligned}\frac{\partial}{\partial t} (\rho_\alpha \, S_\alpha \, \phi) &= S_\alpha \, \phi \, \frac{\partial \, \rho_\alpha}{\partial \, t} + \rho_\alpha \, \phi \, \frac{\partial \, S_\alpha}{\partial \, t} \\ &= S_\alpha \, \phi \, c_\alpha \, \frac{\partial \, p_\alpha}{\partial \, t} + \rho_\alpha \, \phi \, \frac{\partial \, S_\alpha}{\partial \, t} \,,\end{aligned} \tag{2.52}$$

where $c_\alpha = \mathrm{d}\rho_\alpha / \mathrm{d}p_\alpha$ is the compressibility coefficient for phase α. For water $c_\mathrm{w} = \rho_\mathrm{w} \, \beta_\mathrm{w}$. For air c_a is defined by Eq. (2.47). In order to obtain a closed system, one has to make use of the additional relationships discussed in the previous sections. The air saturation is uniquely defined by the water saturation (or vice versa), Eq. (2.8). The water saturation is a function of the capillary pressure, i.e. the difference between the air and water pressures, Eq. (2.13). The relative permeabilities depend on the fluid saturations, and the densities on the fluid pressures, Eqs. (2.46)–(2.47). As a result, a system of two equations with two unknowns is obtained.

Several possibilities exist with respect to the choice of the primary unknown variables. For instance, one can choose the two pressures, p_a and p_w, and compute the capillary pressure and the corresponding fluid saturations accordingly. However, such a formulation is not suitable for the numerical solution, when the air phase disappears completely from the porous medium. In such a situation, the derivatives of the discrete form of the air flow equation are equal to zero. Therefore, it is recommended to choose one of the fluid pressures and one of the saturations as the primary unknowns, e.g.

[31]. As this work focuses on water flow, the water pressure p_w and water saturation S_w are chosen as the primary variables.

Equations (2.50)–(2.51) can be rewritten in order to show explicitly the dependence of each term on the chosen primary variables:

$$\frac{\partial}{\partial t} \left[\rho_w(p_w)\, S_w\, \phi \right] - \nabla \left[\frac{\rho_w(p_w)\, k_s\, k_{rw}(S_w)}{\mu_w} \left(\nabla p_w - \rho_w(p_w)\, \mathbf{g} \right) \right] = 0 \,, \quad (2.53)$$

$$\frac{\partial}{\partial t} \left[\rho_a(p_w, S_w)\, (1 - S_w)\, \phi \right]$$
$$-\nabla \left[\frac{\rho_a(p_w, S_w)\, k_s\, k_{ra}(S_w)}{\mu_a} \left(\nabla p_w + \nabla p_c(S_w) - \rho_a(p_w, S_w)\, \mathbf{g} \right) \right] = 0 \,. \quad (2.54)$$

If the compressibility of the fluids and the porous medium can be neglected, a simplified form of the governing equations is obtained:

$$\phi\, \frac{\partial S_w}{\partial t} - \nabla \mathbf{v}_w = 0 \,, \quad (2.55)$$

$$-\phi\, \frac{\partial S_w}{\partial t} - \nabla \mathbf{v}_a = 0 \,. \quad (2.56)$$

Alternatively, the above equations can be transformed to the fractional flow formulation, e.g. [6]. To this order the mass balance equations are added to each other:

$$\nabla\, (\mathbf{v}_w + \mathbf{v}_a) = \nabla\, \mathbf{v}_t = 0 \,, \quad (2.57)$$

where $\mathbf{v}_t = \mathbf{v}_w + \mathbf{v}_a$ is the total fluid velocity. Equation (2.57) can be rewritten in terms of the fractional flow function f_w and the global pressure p_{glob} defined as follows:

$$f_w = \frac{\lambda_w}{\lambda_w + \lambda_a} \,, \quad (2.58)$$

$$p_{glob} = \frac{1}{2}\, (p_w + p_a) - \int_{S_w^{max}}^{S_w} \left(f_w - \frac{1}{2} \right) \frac{dp_c}{dS_w}\, dS_w \,, \quad (2.59)$$

where S_w^{max} is the maximum water saturation, $p_c(S_w^{max}) = 0$. Equation (2.57) then becomes an elliptic one with respect to the global pressure:

$$\nabla \left\{ k_t \left[\nabla p_{glob} - (f_w\, \rho_w + (1 - f_w)\, \rho_a)\, \mathbf{g} \right] \right\} = 0 \,, \quad (2.60)$$

where:

$$k_t = k_s\, (\lambda_w + \lambda_a) \,. \quad (2.61)$$

Using the definition of the total velocity, the water flux can be expressed as:

$$\mathbf{v}_\mathrm{w} = f_\mathrm{w}\,\mathbf{v}_\mathrm{t} + f_\mathrm{w}\,\lambda_\mathrm{a}\,\mathsf{k}_\mathrm{s}\,(\nabla p_\mathrm{c} + (\rho_\mathrm{w} - \rho_\mathrm{a})\,\mathbf{g})\ . \tag{2.62}$$

Inserting Eq. (2.62) into Eq. (2.55) one obtains the following equation for the water saturation:

$$\phi\frac{\partial S_\mathrm{w}}{\partial t} + \nabla\left[f_\mathrm{w}\,\mathbf{v}_\mathrm{t} + f_\mathrm{w}\,\lambda_\mathrm{a}\,\mathsf{k}_\mathrm{s}\,(\rho_\mathrm{w} - \rho_\mathrm{a})\,\mathbf{g} + f_\mathrm{w}\,\lambda_\mathrm{a}\,\mathsf{k}_\mathrm{s}\,\frac{\mathrm{d}p_\mathrm{c}}{\mathrm{d}S_\mathrm{w}}\,\nabla S_\mathrm{w}\right] = 0\ . \tag{2.63}$$

The above equation has the form of an advection-diffusion one. The first two terms in brackets represent the advective transport. The first term corresponds to the viscous forces, while the second to the gravity forces. The diffusive transport, related to the action of capillary forces, is represented by the third term in brackets. If the capillary and gravity effects are neglected, Eq. (2.63) reduces to the Buckley-Leverett equation (nonlinear advection equation), well known in petroleum reservoir engineering literature, e.g. [13, 31]. In the unsaturated zone, the capillary and gravity forces can rarely be neglected, while the full fractional flow formulation poses problems in the implementation of various types of boundary conditions occurring in unsaturated zone modeling [6]. Moreover, in contrast to the phase pressures, the global pressure is not continuous at the interfaces separating porous materials characterized by different capillary functions. The fractional flow formulation is not used in the numerical simulations presented in the following chapters. However, it will be referred to in the discussion of the general properties of two-phase flow model.

2.2.2 Richards Equation

The two-phase model presented in the previous section can be considerably simplified under specific conditions occurring for air and water flow in the unsaturated zone. At the temperature of 20 °C the air viscosity is about 55 times smaller than the water viscosity, which means that the air mobility is greater than the water mobility by approximately the same factor, if the relative permeabilities of both fluids are similar. Therefore, it can be expected that any pressure difference in the air phase will be equilibrated much faster than in the water phase. On the other hand, it can be often assumed that the air phase is continuous in the pore space and that it is connected to the atmosphere. If the variations in the atmospheric pressure are neglected, one can consider the pore air to be essentially at a constant atmospheric pressure. These assumptions allow to eliminate the equation for the air flow from the system of governing Eqs. (2.50)–(2.51). The capillary pressure is now uniquely defined by the water pressure. For convenience it is often assumed that the reference atmospheric pressure $p_\mathrm{atm} = 0$, so one can write:

$$p_\mathrm{c} = p_\mathrm{atm} - p_\mathrm{w} = -p_\mathrm{w}\ . \tag{2.64}$$

Accordingly, the water saturation and the relative water permeability can be defined as functions of the water pressure. For the values of the water pressure smaller than the negative of the air entry pressure, $p_w < -p_e$ (where p_e can be zero if the van Genuchten capillary function is used), the water saturation and permeability can be computed from the analytical models described in Sect. 2.1.4 and 2.1.6, assuming $p_c = -p_w$. For the values of the water pressure which are larger than the negative of the air entry pressure, $p_w > -p_e$, the water saturation and water permeability are constant and equal to their maximum values.

The remaining equation for the water flow becomes:

$$\frac{\partial}{\partial t} \left(\rho_w \phi \, S_w(p_w) \right) - \nabla \left[\frac{\rho_w(p_w) \, k_s \, k_{rw}(p_w)}{\mu_w} \left(\nabla \, p_w - \rho_w(p_w) \, \mathbf{g} \right) \right] = 0 \, . \quad (2.65)$$

Taking into account Eq. (2.52) the storage term can be rewritten as:

$$\frac{\partial}{\partial t} \left(\rho_w \phi \, S_w \right) = \phi \, S_w \, \rho_w \beta_w \frac{\partial p_w}{\partial t} + \rho_w \phi \, \frac{\partial S_w}{\partial p_w} \frac{\partial p_w}{\partial t} \, . \quad (2.66)$$

Additionally, it is often assumed that the spatial gradients of the water density are negligible:

$$\nabla \left(\rho_w \, \mathbf{v}_w \right) \approx \rho_w \nabla \, \mathbf{v}_w \, .$$

Consequently, both sides of equation can be divided by ρ_w and one arrives at the following form:

$$C_{wp}(p_w) \frac{\partial p_w}{\partial t} - \nabla \left[\frac{k_s \, k_{rw}}{\mu_w} \nabla \, (p_w + \rho_w \, \mathbf{g}) \right] = 0 \, , \quad (2.67)$$

where C_{wp} is a storage coefficient:

$$C_{wp} = \theta_w \, \beta_w + \frac{d\theta_w}{dp_w} \, . \quad (2.68)$$

In hydrological and hydrogeological applications, Eq. (2.67) is often written in terms of the water pressure head:

$$C_{wh}(h_w) \frac{\partial h_w}{\partial t} - \nabla \left[K_{sw} \, k_{rw}(h_w) \nabla \, (h_w + z) \right] = 0 \, , \quad (2.69)$$

where $C_{wh} = \rho_w \, g \, C_{wp}$. Accordingly, the capillary and relative permeability functions are defined in terms of the capillary pressure head, which is equal to the negative water pressure head. Equations (2.67) and (2.69) describe transient water flow in both saturated and unsaturated conditions and are sometimes called generalized Richards equation.

By further neglecting the water compressibility one arrives at the following equation:

$$C_{\text{ch}}(h_{\text{w}}) \frac{\partial h_{\text{w}}}{\partial t} - \nabla \left[\mathsf{K}_{\text{sw}} \, k_{\text{rw}}(h_{\text{w}}) \nabla \, (h_{\text{w}} + z) \right] = 0 \, , \qquad (2.70)$$

where the storage coefficient accounts only for the changes in water saturation:

$$C_{\text{ch}}(h_{\text{w}}) = \phi \, \frac{\mathrm{d}S_{\text{w}}}{\mathrm{d}h_{\text{w}}} = \frac{\mathrm{d}\theta_{\text{w}}}{\mathrm{d}h_{\text{w}}} \, . \qquad (2.71)$$

This coefficient is often called specific water (or moisture) capacity, e.g. [85].

Equation (2.70) was originally developed by Richards [65], while the corresponding expression for the water flux in unsaturated conditions:

$$\mathbf{v}_{\text{w}} = -\mathsf{K}_{\text{sw}} \, k_{\text{rw}}(h_{\text{w}}) \nabla \, (h_{\text{w}} + z) \qquad (2.72)$$

was suggested earlier by Buckingham [8] and is often called Darcy-Buckingham equation, e.g. [55]. In saturated conditions $C_{\text{ch}} = 0$ and Eq. (2.70) degenerates to an elliptic equation describing steady flow. Thus a generalized form of the Richards equation, which includes water compressibility, Eq. (2.69), is preferable if parabolic character of the governing equation is to be retained during transition between saturated and unsaturated states. In geotechnical and hydrogeological applications, Eq. (2.69) is often modified by accounting for the compressibility of the solid skeleton in the storage term $\phi = \phi(p_{\text{w}}, p_{\text{a}})$. These effects are not considered here, as they are not essential for the analyses presented in the following chapters.

Equation (2.70) is often referred to as the pressure-based form of the Richards equation. Alternatively it can be rewritten in the so-called mixed form, which includes explicitly both the water content and the water pressure head:

$$\frac{\partial \theta (h_{\text{w}})}{\partial t} - \nabla \left[\mathsf{K}_{\text{sw}} \, k_{\text{rw}}(h_{\text{w}}) \, \nabla \, (h_{\text{w}} + z) \right] = 0 \, . \qquad (2.73)$$

It was shown that the mixed form has better properties with respect to the numerical solution, as it allows to minimize the mass balance error, persistent in the solutions employing the pressure-based form [12]. The third possible form is obtained by replacing the pressure head in all terms of Eq. (2.73) with the water content. To this order the hydraulic diffusivity tensor is introduced:

$$\mathsf{D}(\theta_{\text{w}}) = \frac{\mathrm{d}h_{\text{w}}}{\mathrm{d}\theta_{\text{w}}} \, \mathsf{K}_{\text{sw}} \, k_{\text{rw}}(\theta_{\text{w}}) \, , \qquad (2.74)$$

so that Eq. (2.73) becomes:

$$\frac{\partial \theta_w}{\partial t} - \nabla \left[\mathsf{D} \left(\theta_w \right) \nabla \theta_w \right] + \mathsf{K}_{sw} \, k_{rw}(\theta_w) \, \nabla z = 0 \ . \tag{2.75}$$

Note that the above equation can be obtained as the limit case of the saturation equation in the fractional flow model, Eq. (2.63), assuming that the air phase is much more mobile than the water phase, $\lambda_a \gg \lambda_w$, and that the air phase density is much smaller than the water density $\rho_a \ll \rho_w$. In this case the relevant terms of Eq. (2.63) become:

$$f_w = \frac{\lambda_w}{\lambda_a + \lambda_w} \approx 0 \ , \tag{2.76}$$

$$f_w \, \lambda_a = \frac{\lambda_w \, \lambda_a}{\lambda_a + \lambda_w} \approx \lambda_w = \frac{k_{rw}}{\mu_w} \ , \tag{2.77}$$

$$\phi \frac{\partial S_w}{\partial t} = \frac{\partial \theta_w}{\partial t} \ , \tag{2.78}$$

$$f_w \, \mathbf{v}_t \approx 0 \ , \tag{2.79}$$

$$f_w \, \lambda_a \, \mathsf{k}_s \, (\rho_w - \rho_a) \, \mathbf{g} \approx \lambda_w \, \mathsf{k}_s \, \rho_w \, \mathbf{g} = -\mathsf{K}_{sw} \, k_{rw} \, \nabla z \ , \tag{2.80}$$

$$f_w \, \lambda_a \, \mathsf{k}_s \, \frac{\mathrm{d}p_c}{\mathrm{d}S_w} \, \nabla S_w \approx \lambda_w \, \mathsf{k}_s \, \frac{\mathrm{d}p_c}{\mathrm{d}S_w} \, \nabla S_w = -\mathsf{K}_{sw} \, k_{rw} \, \frac{\mathrm{d}h_w}{\mathrm{d}\theta_w} \, \nabla \theta_w \ . \tag{2.81}$$

The above assumptions lead to Eq. (2.75).

The water content (or saturation) based form is easier to solve numerically than the mixed or pressure based forms. Due to its similarity to the standard advection-diffusion equation it is often used to obtain analytical or semi-analytical solutions of the Richards equation, especially for one-dimensional flow, where the diffusivity and conductivity coefficients are scalars. The major drawback of the water-content based form is that it becomes indefinite in fully saturated conditions. Additional difficulty arises when the domain under consideration contains porous regions characterized by different capillary functions, because the water content is not continuous at such interfaces (see Sect. 2.3.3).

Yet another form of the Richards equation can be obtained for an isotropic medium using the Kirchhoff transform. The Kirchhoff variable, also called the flux potential can be defined as (e.g. [36, 85]):

$$\Phi_h(h_w) = \int\limits_{-\infty}^{h_w} k_{rw}(\hat{h}) \, \mathrm{d}\hat{h} \ , \tag{2.82}$$

where $\hat{h}$ is the integration variable. Using this transformation, the Richards equation can be rewritten as follows:

$$\phi \frac{\mathrm{d}S_\mathrm{w}}{\mathrm{d}\Phi_\mathrm{h}} \frac{\partial \Phi_\mathrm{h}}{\partial t} - \nabla \left(\mathsf{K}_\mathrm{sw} \nabla \Phi_\mathrm{h} \right) + \mathsf{K}_\mathrm{sw} k_\mathrm{rw}(\Phi_\mathrm{h}) \nabla z = 0 \, . \tag{2.83}$$

Alternatively, the flux potential can be also defined with respect to the water pressure as the primary variable:

$$\Phi_\mathrm{p}(p_\mathrm{w}) = \int\limits_{-\infty}^{p_\mathrm{w}} k_\mathrm{rw}(\hat{p}) \, \mathrm{d}\hat{p} \, . \tag{2.84}$$

Similarly to the water content, the flux potential is not continuous at material interfaces. Nevertheless, Eq. (2.83) is easier to solve numerically than the mixed and pressure-based forms of the Richards equation, and in contrast to the saturation-based form, can be used for fully saturated conditions. Several authors proposed efficient numerical algorithms based on this form of the Richards equation, e.g. [5, 36, 67]. Moreover, even if the mixed or pressure-based form of the Richards equation is solved, the Kirchhoff transform can be a useful tool to approximate the effective conductivity between the adjacent nodes (see Chap. 4).

While the Richards equation is a widely accepted model for the water flow in unsaturated soils and rocks, one has to be aware of its limitations. For obvious reasons, it cannot be used when there is an explicit interest in the simulation of air flow. Such applications include for example transport of volatile contaminants in the pore air, e.g. [11, 78], or dewatering by means of compressed air used in tunnel construction, e.g. [57]. However, even if the primary interest is in the water flow, the Richards equation can lead to inaccurate results, if one or more of the underlying assumptions is not fulfilled, as pointed out by several studies, e.g. [50, 51, 60, 80, 83, 84].

A number of sources for the possible discrepancies between the Richards model and the full two-phase model can be identified. The first one is related to the viscosity ratio between air and water. Numerical experiments [73] showed that the agreement between results obtained from the Richards equation and from the two-phase model is less than perfect for the water-to-air viscosity ratio smaller than 100. In natural conditions the viscosity of air can be expected to be only about 50 to 60 times smaller than the mobility of water. It should be noted that the phase mobility depends not only on its viscosity, but also on the relative permeability. Thus, further decrease in the mobility ratio can be expected if the relative permeability of air is much smaller than the permeability of water, which occurs as the air saturation approaches the residual value. For instance, it was shown that significant differences arise between the Richards model and the two-phase flow model if the relative permeabilities of water and air are proportional to the fourth power of the respective saturation, even assuming the viscosity ratio of the fluids equal to 100 [19].

The second factor limiting the applicability of the Richards equation is the presence of obstacles, which do not allow the pore air to contact freely with the atmospheric air. Examples of such obstacles include layers of porous media which are quasi-impermeable to air, either because they have very low intrinsic

permeability, or because they are saturated or nearly saturated with water. In this context, inadequacy of the Richards equation was demonstrated for various types of problems, such as infiltration in columns with sealed bottom [74–76], drainage of coarse sand overlaid by a layer of fine sand [40], field-scale infiltration with shallow groundwater table [27], increase of the water level in wells during ponded infiltration [26], or air trapping in flood embankments due to overtopping by flood wave [46]. The flowpaths of the pore air can also be blocked due to heterogeneous structure of the porous medium, especially if coarse-textured inclusions with low air entry pressure are embedded in a fine-textured background having high entry pressure. Such effects are investigated in Chap. 7.

2.2.3 Single-Phase Flow

Single phase flow occurs when the pores are completely filled with only one fluid phase, which in the context of this work is water. Since $S_w = 1$ and $k_{rw} = 1$, the governing equation for the water flow becomes:

$$\frac{\partial}{\partial t} (\rho_w \phi) - \nabla \left[\frac{\rho_w \, \mathsf{k}_{sw}}{\mu_w} (\nabla \, p_w - \rho_w \, \mathbf{g}) \right] = 0 \; . \tag{2.85}$$

Similarly to the case of the Richards equation, saturated groundwater flow is usually described in terms of the water pressure head. Moreover, the spatial gradients of the water density are neglected, resulting in the following equation:

$$C_{sat} \frac{\partial h_w}{\partial t} - \nabla \left[\mathsf{K}_{sw} \nabla \, (h_w + z) \right] = 0 \; , \tag{2.86}$$

where the saturated storage coefficient $C_{sat} = \rho_w \, \beta_w \, g \, \phi$ is approximately constant. The above equation is valid for a rigid solid skeleton. In groundwater aquifers the compressibility of the skeleton is usually more important than the compressibility of water and has to be accounted for in the storage coefficient, e.g. [16].

It is important to note that when porous media are subject to imbibition in natural conditions, the transition from the unsaturated to fully saturated state occurs not directly, but via the occluded air bubble regime. At this stage the Darcy-scale capillary pressure is considered constant and equal to its minimum value (p_e^{wet} in Fig. 2.4, which can be equal to zero in many cases), while the water pressure assumes values above $-p_e^{wet}$. However, the water saturation can further increase due to compressibility of the air bubbles, even though the macroscopic capillary pressure remains equal to zero for positive values of the water pressure. Moreover, the increase of the water saturation causes an increase in the relative permeability. While this effects are often neglected and the water saturation and permeability are assumed to be constant for the whole range of positive water pressures, the additional compressibility of the medium resulting from the presence of air bubbles can be important,

for example when considering soil liquefaction due to rapidly oscillating loading, e.g. [35].

2.3 Auxiliary Conditions

The governing equations for the two-phase (Eqs. (2.50)–(2.51)), unsaturated (Eq. (2.65)) or single-phase (Eq. (2.85)) unsteady flow in porous media are partial differential equations of parabolic type [31, 63]. These equations are solved in the spatial domain W, as shown schematically in Fig. 2.7 and for the time interval $\langle 0, t_{\max}\rangle$. The solution problem should be well-posed, which means that the following conditions are satisfied, e.g. [18, 71]:

- the solution exists,
- the solution is unique,
- the solution depends continuously on the initial and boundary conditions.

In order to obtain a well-posed problem, the initial and boundary conditions must be formulated in an appropriate manner. The initial conditions specify the state of the system at time $t = 0$, while the boundary conditions determine the behaviour of the unknown functions at the external boundaries ∂W of the considered spatial domain. For parabolic equations the boundary conditions can be in general time-dependent. In the case of steady flow, the derivatives with respect to time disappear from the governing equations and the equations become elliptic. For such type of equations, only boundary conditions are required and they are independent of time.

Moreover, porous materials in the solution domain may be heterogeneous with respect to the constitutive parameters and relationships such as the absolute permeability or the capillary and relative permeability functions. In general, one can assume either that the spatial domain is composed of several porous regions separated by internal boundaries (material interfaces), with uniform parameter distribution in each region, or that the parameters are continuously variable in space. In the first case the mathematical formulation must be complemented by additional conditions for the material interfaces, which allow to link the solutions from the neighbouring sub-domains. In the case of continuous distribution, a similar problem arises during numerical solution of the governing equations when spatial discretization is performed and specific material properties are assigned to each element of the grid.

2.3.1 Initial Conditions

The initial state of the system can be defined either in terms of the primary variables, or in terms of other variables, from which the primary ones can be calculated. For two-phase flow in the p_{w}–S_{w} formulation, the initial conditions can be specified as:
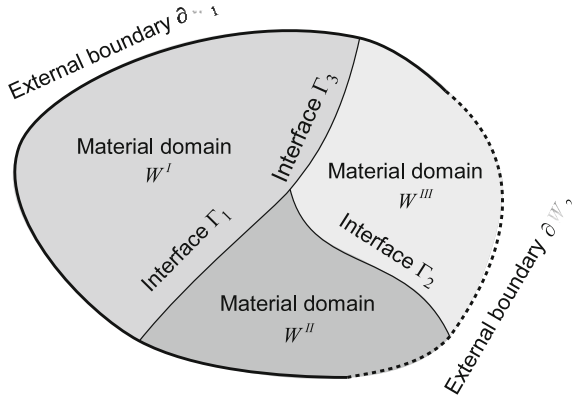
Fig. 2.7 Solution domain for flow equations with external and internal boundaries

$$p_{\mathrm{w}}(\mathbf{x}, t = 0) = p_{\mathrm{w}}^{\mathrm{init}}(\mathbf{x}) , \tag{2.87}$$

$$S_{\mathrm{w}}(\mathbf{x}, t = 0) = S_{\mathrm{w}}^{\mathrm{init}}(\mathbf{x}) . \tag{2.88}$$

In strictly unsaturated conditions, the initial water pressure can be replaced by the initial air pressure $p_{\mathrm{a}}^{\mathrm{init}}(\mathbf{x})$. However, if part of the domain is fully saturated with water, the air pressure cannot be meaningfully defined. On the other hand, it is also possible to define the initial conditions in terms of the two pressures:

$$p_{\mathrm{w}}(\mathbf{x}, t = 0) = p_{\mathrm{w}}^{\mathrm{init}}(\mathbf{x}) , \tag{2.89}$$

$$p_{\mathrm{a}}(\mathbf{x}, t = 0) = p_{\mathrm{a}}^{\mathrm{init}}(\mathbf{x}) . \tag{2.90}$$

The water saturation is then computed as $S_{\mathrm{w}}^{\mathrm{init}} = S_{\mathrm{w}}(p_{\mathrm{a}}^{\mathrm{init}} - p_{\mathrm{w}}^{\mathrm{init}})$. For the Richards model, only the initial value of the water pressure is necessary:

$$p_{\mathrm{w}}(\mathbf{x}, t = 0) = p_{\mathrm{w}}^{\mathrm{init}}(\mathbf{x}) . \tag{2.91}$$

In strictly unsaturated conditions it is possible to use initial distribution of saturation. The corresponding values of the water pressure are then obtained from the capillary function $p_{\mathrm{w}}^{\mathrm{init}} = -p_{\mathrm{c}}(S_{\mathrm{w}}^{\mathrm{init}})$.

While the initial distribution of the relevant variables can be obtained from measurements, it is common to assume some simple distribution schemes, for example:

- Uniform water and air pressures:

$$p_{\mathrm{w}}(\mathbf{x}, t = 0) = p_{\mathrm{w}}^{\mathrm{init}} , \tag{2.92}$$

$$p_{\mathrm{a}}(\mathbf{x}, t = 0) = p_{\mathrm{a}}^{\mathrm{init}} , \tag{2.93}$$

$$S_{\mathrm{w}}(\mathbf{x}, t = 0) = S_{\mathrm{w}}(p_{\mathrm{a}} - p_{\mathrm{w}}) . \tag{2.94}$$

In a homogeneous medium, uniform pressure distribution implies uniform distribution of the water saturation. In a heterogeneous medium, the values of water saturation will be different in each material region. If the gravity force is present in the system then some initial flow occurs due to the presence of gradient in the gravity potential. Otherwise the system is at equilibrium.

- Uniform water saturation:

$$S_w(\mathbf{x}, t = 0) = S_w^{\text{init}}. \tag{2.95}$$

This condition must be completed by specifying either water or air pressure. Particular attention is required if such a condition is applied to a heterogeneous medium. For fully water saturated domain, a natural choice is to use $S_w^{\text{init}} = 1$ or $S_w^{\text{init}} = 1 - S_{\text{ra}}$ and assume a uniform or hydrostatic distribution of the water pressure. If the medium is characterized by spatially varying entry pressure values, the corresponding distribution of the capillary pressure is discontinuous. On the other hand, in unsaturated conditions it is common to assume a uniform initial value of the air pressure equal to the atmospheric pressure. In this case spatial variability of the capillary function results in a discontinuous initial distribution of the water pressure and implies initial water flow between adjacent material regions.

- Hydrostatic water and air pressure distributions:

$$p_w(\mathbf{x}, t = 0) = p_w^{\text{ref}} + \rho_w \, g \, z \tag{2.96}$$

$$p_a(\mathbf{x}, t = 0) = p_a^{\text{ref}} + \rho_a \, g \, z \tag{2.97}$$

$$S_w(\mathbf{x}, t = 0) = S_w(p_a - p_w) \tag{2.98}$$

This case describes a system in equilibrium. It is often applied if the position of the groundwater table is known. The compressibility effects are assumed unimportant.

- Hydrostatic water pressure and uniform air pressure

$$p_w(\mathbf{x}, t = 0) = p_w^{\text{ref}} + \rho_w \, g \, z \tag{2.99}$$

$$p_a(\mathbf{x}, t = 0) = p_{\text{atm}} \tag{2.100}$$

$$S_w(\mathbf{x}, t = 0) = S_w(p_a - p_w) \tag{2.101}$$

Since the variations in the air pressure due to gravity are relatively small, they are often neglected. If the atmospheric air pressure is assumed everywhere in the domain, the vertical saturation profile above the water table corresponds exactly to the capillary function drawn in S_w–h_c coordinates. There is some initial air flow, but it is negligibly small.

2.3.2 Boundary Conditions

Boundary conditions provide information about the behaviour of the solution at physical boundaries of the domain. In general three types of the boundary conditions are distinguished, e.g. [63, 87]:

1. Dirichlet boundary conditions specify the values of the solution at a given part of the boundary;
2. Neumann boundary conditions specify the value of the spatial derivative of the solution. In the case of flow in porous media, this type of condition is usually written in terms of the fluid flux in the direction normal to the boundary;
3. Robin boundary conditions, which specify a relationship between the value of solution and its derivative, and can be viewed as a generalization of both Dirichlet and Neumann boundary conditions.

various boundary conditions can be specified on different parts of the domain boundary. For a steady flow problem, described by an elliptic equation, it is necessary to provide Dirichlet boundary conditions on at least one point of the boundary, otherwise the problem becomes ill-posed. For unsteady problems, described by parabolic equations, no such restriction exists. In the case of two-phase flow it is necessary to specify boundary conditions for each phase, and different types of condition can be used for each fluid at the same part of the boundary. Some examples of boundary conditions typically used in unsaturated flow modelling are listed below.

Dirichlet boundary conditions provide values of the pressures and/or saturations of the two fluid phases. They are typically applied when:

- the water pressure is known, e.g.:
  - the boundary corresponds to the groundwater table,
  - the distance between the boundary and the groundwater table is known, and a hydrostatic distribution of the water pressure between them can be assumed,
  - the boundary is in contact with a free water body assumed to be static, e.g. at the waterward slope of a dike or at the soil surface ponded by a water layer,
  - a specific negative value of the water pressure is applied, e.g. during infiltration or drainage experiments in controlled conditions,

- the air pressure is known, e.g. the boundary is exposed to the atmosphere and not fully water saturated,
- the water saturation is known, e.g. the boundary is fully saturated and the air pressure cannot be meaningfully specified,
- the boundary is far away from the region of interest and it can be assumed that the water and air pressures and saturations are constant and equal to the initial ones.

Neumann boundary conditions are typically used when the boundary is impermeable for one or both phases, $\rho_\alpha \, \mathbf{v}_\alpha \, \mathbf{n}_W = 0$, where $\mathbf{n}_W$ is a unit vector normal to the boundary of the domain W. This condition is also used to represent infiltration and evaporation fluxes at the soil surface.
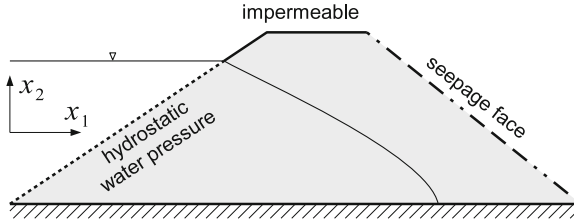
Fig. 2.8 Boundary conditions for a simple case of two-dimensional flow in a dike

Moreover, there are three specific sets of the boundary conditions widely applied in the unsaturated zone modelling. They include the free drainage condition, the seepage face condition and the soil-atmosphere interface condition e.g. [64, 72]. All of them are system-dependent, which means that the imposed value of the pressure of flux depends on the current state of the system. The free drainage condition represents vertical flow of water through the bottom of the soil profile towards a distant groundwater table. It is assumed that the water pressure gradient is zero and only the gravity component contributes to the flow:

$$\mathbf{v}_\text{w}\,\mathbf{n}_W = \left(\frac{\rho_\text{w}}{\mu_\text{w}}\mathsf{k}_\text{w}(S_\text{w})\,\mathbf{g}\right)\,\mathbf{n}_W \qquad (2.102)$$

Thus, the condition is of Neumann type, but the actual value of the flux depends on the solution at the specific boundary point.

The seepage face is a part of the outer surface of the porous medium which is exposed to the atmosphere and through which water can flow freely out of the porous domain. It typically occurs above the water level in wells and at the bottom of the landward slopes of earth dams or embankments, Fig. 2.8. The seepage face is considered impermeable to water as long as the adjacent part of the porous medium is unsaturated. If the pressure in the medium increases to the value of the atmospheric pressure water flows out freely from the medium and no build-up of positive pressure values is allowed. This is represented by assuming Neumann boundary condition $\mathbf{v}_\text{w}\,\mathbf{n}_W = 0$ on the unsaturated part of the boundary and Dirichlet boundary condition $p_\text{w} = 0$ on the saturated part. The position of the saturated-unsaturated interface is not known a priori and must be obtained iteratively during the numerical solution.

When modelling the infiltration and evaporation processes at the soil surface, it is often necessary to switch between Neumann and Dirichlet boundary condition, depending on the state of soil surface. During infiltration, at first a specific value of the water flux is applied at the boundary, Fig. 2.9a. As a result of the infiltration the water pressure at the soil surface increases from the initially negative value towards zero (atmospheric pressure). If the applied flux is larger than the soil infiltration capacity (equal to the saturated water conductivity) then positive values of the water pressure appear at the surface, which physically corresponds to the formation of a water layer on the ground surface (ponding). At this point the boundary condition for
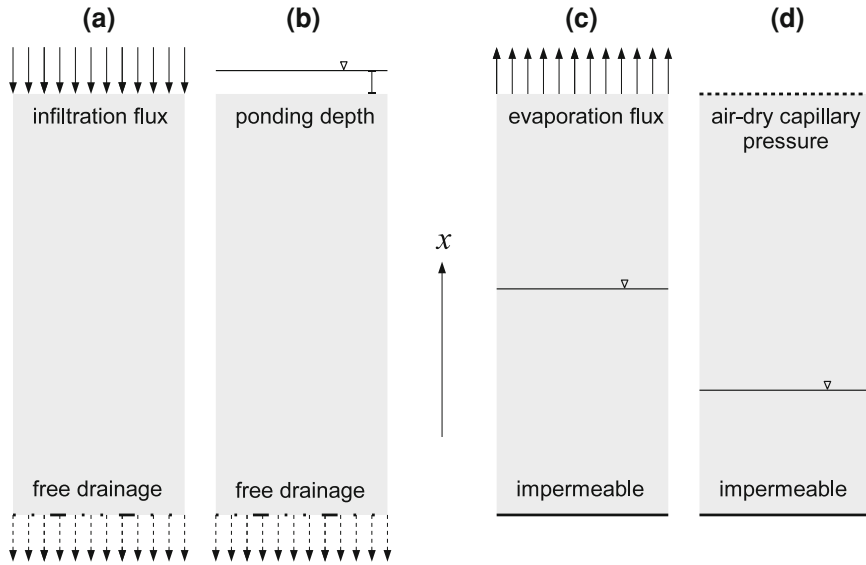
Fig. 2.9 Boundary conditions for typical one-dimensional flow problems: infiltration towards a distant groundwater table, **a** early stage, **b** late stage; evaporation from shallow groundwater table, **c** early stage, **d** late stage

the water phase is switched to Dirichlet type ($p_w = 0$ or some small positive value) and it is assumed that the excess precipitation forms the surface runoff, Fig. 2.9b. If the precipitation rate decreases below the soil infiltration capacity, the condition is switched back to Neumann type. A similar switch in the boundary conditions is performed when modelling evaporation. In this case the water pressure at the surface decreases as the water evaporates from soil at a specific rate, Fig. 2.9c. However, the water pressure cannot fall below a limit value defined by the temperature and relative humidity of the air, p_{dry}. If this value is reached, the boundary condition is switched to Dirichlet type with $p_w = p_{dry}$ and is maintained until the potential evaporation rate decreases or a rainfall occurs, Fig. 2.9d. It should be noted that such an approach provides only simplified description of the soil-atmosphere interface and is used primarily with the Richards model. More sophisticated modelling concepts are based on the coupling of air and water flow in porous medium with free flow of the surface water (after ponding) or atmospheric air above the soil-atmosphere interface, e.g. [22, 52].

2.3.3 Conditions at Material Interfaces

Porous media often consist of multiple regions, each of them having different properties such as porosity, intrinsic permeability, capillary function and relative
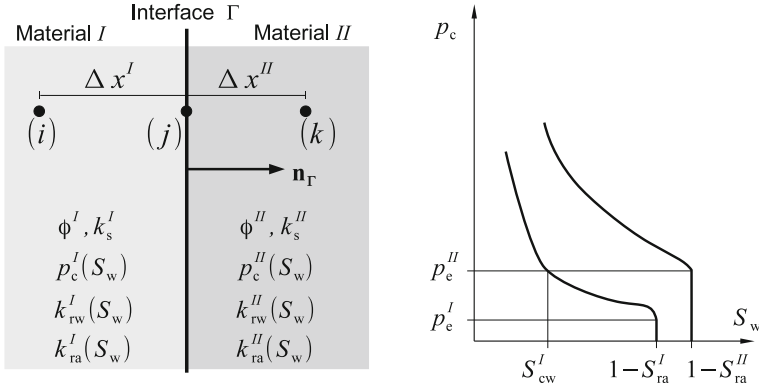
Fig. 2.10 Conditions at material interface separating two porous media

permeability functions. In each region the fluid flow is described by Eqs. (2.50)–(2.51), or by Eq. (2.65). The solutions in different subdomains must be connected to each other by appropriate interface conditions [30, 31].

Consider an interface between two porous materials, as shown in Fig. 2.10. At the Darcy's scale, the interface can be considered infinitely thin. Thus, the mass conservation principle implies that for each phase the components of the mass fluxes in the direction normal to the interface are equal:

$$(\rho_\alpha \mathbf{v}_\alpha)^I \mathbf{n}_\Gamma = (\rho_\alpha \mathbf{v}_\alpha)^{II} \mathbf{n}_\Gamma \tag{2.103}$$

where $\mathbf{n}_\Gamma$ is a unit vector normal to the interface Γ and oriented from material I to material II.

The second interface condition can be derived from the principle of momentum conservation [30], and states the continuity of the pressures in the two fluid phases, and consequently the continuity of the capillary pressure:

$$p_w^I = p_w^{II} \tag{2.104}$$

$$p_a^I = p_a^{II} \tag{2.105}$$

$$p_c^I = p_c^{II} \tag{2.106}$$

Note that the continuity of the capillary pressure implies that the water and air saturations are discontinuous, except for the case of two media characterized by the same capillary function. Moreover, if the saturation on one side of the interface is known, the saturation at the opposite side can be computed from the capillary pressure continuity condition:

$$S_w^I = S_w^I \left(p_c^{II} \left(S_w^{II} \right) \right) \tag{2.107}$$

The above conditions hold if both fluid phases are continuous in the pore space at each side of the interface. A special case arises if the one of the materials, say material *II*, is characterized by a distinct air entry pressure, higher than the entry pressure of the other material. As the value of p_e^{II} is reached, the air (or non-wetting fluid in general) is no longer continuous, and the macroscopic capillary pressure remains at its minimum value. At the other side of the interface, the capillary pressure can assume smaller values, or even reach zero if $p_e^{I} = 0$. The state of the system can be meaningfully defined by the capillary pressure p_c^{I} or the corresponding water saturation S_w^{I}. On the other hand, the state of the material (I) cannot be uniquely determined by the saturation or the capillary pressure in material (II). In such a situation, the extended capillary pressure condition can be formulated as [15]:

$$
\begin{cases}
p_c^I(S_w^I) = p_c^{II}(S_w^{II}) & \text{if } S_w^I < S_{cw}^I \\
S_w^{II} = 1 - S_{ra}^{II} & \text{if } S_w^I \geq S_{cw}^I
\end{cases}
\tag{2.108}
$$

where the threshold saturation at the left side of the interface S_{cw}^I corresponds to the entry pressure of the material at the right-hand side, $S_{cw}^I = S_w^I(p_e^{II})$. At the same time, the pressure continuity condition for the water phase (2.104) holds, as the water phase is continuous at both sides of the interface.

In the case of the Richards equation, only conditions for the water phase have to be formulated at the interface. They include the continuity of the normal flux and continuity of the water pressure. The water saturation, now uniquely defined by the water pressure, is in general discontinuous at the interfaces. The interface conditions must be properly taken into account in the development of spatial discretization schemes for both two-phase model and the Richards equation, as it will be shown in the following chapter.

Application of the pressure and flux continuity conditions for the case of single-phase flow leads to the well known formula for the equivalent permeability of a layered medium in the direction perpendicular to the layers. Assuming that the values of the water pressure at points i, j and k are known, one can write:

$$
-k_s^I \frac{p^{I(j)} - p^{(i)}}{\Delta x^I} = -k_s^{II} \frac{p^{(k)} - p^{II(j)}}{\Delta x^{II}} = -k_s^{eq} \frac{p^{(k)} - p^{(i)}}{\Delta x^I + \Delta x^{II}}
\tag{2.109}
$$

where k_s^{eq} is the equivalent intrinsic permeability and by virtue of the pressure continuity $p^{I(j)} = p^{II(j)}$. Solving the above double equation, one can express the equivalent permeability as a weighted harmonic average of the permeabilities of the two materials:

$$
k_s^{eq} = \frac{(\Delta x^I + \Delta x^{II}) k_s^I k_s^{II}}{\Delta x^I k_s^{II} + \Delta x^{II} k_s^I}
\tag{2.110}
$$

This formula will be used in the subsequent chapters to develop spatial discretization schemes for both homogeneous and heterogeneous porous media.

References

1. Auriault JL (1987) Nonsaturated deformable porous media: Quasistatics. Transport in Porous Media 2(1):45–64, 10.1007/BF00208536
2. Auriault JL, Boutin C, Geindreau C (2009) Homogenization of coupled phenomena in heterogeneous media. Wiley, Hoboken
3. Baker D (1995) Darcian weighted interblock conductivity means for vertical unsaturated flow. Ground Water 33(3):385–390, 10.1111/j.1745-6584.1995.tb00294.x
4. Bear J (1972) Dynamics of fluids in porous media. Elsevier, Amsterdam
5. Berninger H, Kornhuber R, Sander O (2011) Fast and robust numerical solution of the Richards' equation in homogeneous soil. SIAM Journal on Numerical Analysis 49(6):2576–2597, 10.1137/100782887
6. Binning P, Celia M (1999) Practical implementation of the fractional flow approach to multi-phase flow simulation. Advances in Water Resources 22(5):461–478, 10.1016/S0309-1708(98)00022--0
7. Brooks R, Corey A (1964) Hydraulic properties of porous media. Tech. rep., Hydrology Paper 3, Colorado State University, Fort Collins, Colorado, USA
8. Buckingham E (1907) Studies on the movement of soil moisture. Tech. rep., Bulletin 38 U.S. Department of Agriculture Bureau of Soils
9. Burdine N (1953) Relative permeability calculations from pore size distribution data. Transactions of the American Institute of Mining, Metallurgical and Petroleum Engineers 198:71–77
10. Carsel R, Parrish R (1988) Developing of joint probability distributions of soil water retention characteristics. Water Resources Research 24(5):755–769, 10.1029/WR024i005p00755
11. Celia M, Binning P (1992) A mass conservative numerical solution for two-phase flow in porous media with application to unsaturated flow. Water Resources Research 28(10):2819–2828, 10.1029/92WR01488
12. Celia M, Bouloutas E, Zarba R (1990) A general mass-conservative numerical solution for the unsaturated flow equation. Water Resources Research 26(7):1483–1496, 10.1029/WR026i007p01483
13. Chen Z, Huan G, Ma Y (2006) Computational methods for multiphase flows in porous media. SIAM, Philadelphia
14. Darcy H (1856) Les fontaines publiques de la ville de Dijon. Dalmont, Paris
15. de Neef M, Molenaar J (1997) Analysis of DNAPL infiltration in a medium with a low permeable lens. Computational Geosciences 1(2):191–214, 10.1023/A:1011569329088
16. Domenico P, Schwartz F (1998) Physical and chemical hydrogeology. Wiley, New York
17. Feddes R, de Rooij G, van Dam J (eds) (2004) Unsaturated-zone modeling: progress, challenges and applications. Kluwer, Dordrecht
18. Fletcher C (1991) Computational techniques for fluid dynamics 1. Fundamental and general techniques, Springer, Berlin
19. Forsyth P (1988) Comparison of the single-phase and two-phase numerical model formulation for saturated-unsaturated groundwater flow. Computer Methods in Applied Mechanics and Engineering 69(2):243–259
20. Fredlund D, Rahardjo H (1993) Soil mechanics for unsaturated soils. Wiley, New York
21. Fredlund D, Xing A (1994) Equations for the soil-water characteristic curve. Canadian Geotechnical Journal 31(4):521–532, 10.1139/t94-061
22. Furman A (2008) Modeling coupled surface-subsurface flow processes: A review. Vadose Zone Journal 7(2):741–756, 10.2136/vzj2007.0065
23. Gardner W (1958) Some steady-state solutions of the unsaturated moisture flow equation with the application to evaporation from a water table. Soil Science 85(4):228–232
24. Gawin D, Baggio P, Schrefler B (1995) Coupled heat, water and gas flow in deformable porous media. International Journal for Numerical Methods in Fluids 20:969–987
25. Gray W, Hassanizadeh S (1991) Paradoxes and realities in unsaturated flow theory. Water Resources Research 27(8):1847–1854, 10.1029/91WR01259

26. Guo H, Jiao J, Weeks E (2008) Rain-induced subsurface airflow and Lisse effect. Water Resources Research 44:W07409,10.1029/2007WR006294
27. Hammecker C, Antonino A, Maeght J, Boivin P (2003) Experimental and numerical study of water flow in soil under irrigation in northern senegal: evidence of air entrapment. European Journal of Soil Science 54:491–503
28. Hassanizadeh M, Gray W (1980) General conservation equations for multi-phase systems: 3. Constitutive theory for porous media flow. Advances in Water Resources 3(1):25–40,10.1016/0309-1708(80)90016--0
29. Hassanizadeh M, Gray W (1993) Toward an improved description of the physics of two-phase flow. Advances in Water Resources 16(1):53–67,10.1016/0309-1708(93)90029-F
30. Hassanizadeh S, Gray W (1989) Boundary and interface conditions in porous media. Water Resources Research 25(7):1705–1715,10.1029/WR025i007p01705
31. Helmig R (1997) Multiphase flow and transport processes in the subsurface: a contribution to the modeling of the hydrosystems. Springer, Berlin
32. Hilfer R (2006) Capillary pressure, hysteresis and residual saturation in porous media. Physica A 359:119–128
33. Hillel D (1998) Environmental soil physics. Academic Press, San Diego, California
34. Ippisch O, Vogel HJ, Bastian P (2006) Validity limits for the van Genuchten—Mualem model and implications for parameter estimation and numerical simulation. Advances in Water Resources 29(12):17801789,10.1016/j.advwatres.2005.12.011
35. Ishihara K, Tsukamoto Y, Nakazawa H, Kamada K, Huang Y (2002) Resistance of partly saturated sand to liquefaction with reference to longitudinal and shear wave velocities. Journal of Soils and Foundations, JGS 42:6
36. Ji SH, Park YJ, Sudicky E, Sykes J (2008) A generalized transformation approach for simulating steady-state variably-saturated subsurface flow. Advances in Water Resources 31(2):313–323,10.1016/j.advwatres.2007.08.010
37. Khlosi M, Cornelis W, Douaik A, van Genuchten M, Gabriels D (2008) Performance evaluation of models that describe the soil water retention curve between saturation and oven dryness. Vadose Zone Journal 7(1):87–96,10.2136/vzj2007.0099
38. Kosugi K, Hopmans J, Dane J (2002) Parametric models. In: JH D, GC T (eds) Methods of soil analysis. Part 4: Physical methods, Soil Science Society of America, Inc., Madison, Wisconsin, pp 739–757
39. Kovács G (1981) Seepage hydraulics. Elsevier, Amsterdam
40. Kuang X, Jiao J, Wan L, Wang X, Mao D (2011) Air and water flows in a vertical sand column. Water Resources Research 47:W04506,10.1029/2009WR009030
41. Kutílek M, Nielsen D (1994) Soil hydrology. Catena , Cremlingen
42. Lassabatere L, Angulo-Jaramillo R, Soria Ugalde J, Cuenca R, Braud I, Haverkamp R (2006) Beerkan estimation of soil transfer parameters through infiltration experiments - BEST. Soil Science Society of America Journal 70(2):521–532,10.2136/sssaj2005.0026
43. Leij F, Russel W, Lesch S (1997) Closed-form expressions for water retention and conductivity data. Ground Water 35(5):848–858,10.1111/j.1745-6584.1997.tb00153.x
44. Lenhard R, Parker J, Mishra S (1989) On the correspondence between Brooks-Corey and van Genuchten models. Journal of Irrigation and Drainage Engineering ASCE 115:744–751
45. Leong EC, Rahardjo H (1997) Review of soil-water characteristic curve equations. Journal of Geotechnical and Geoenvironmental Engineering 123(12):1106–1117
46. Lesniewska D, Zaradny H, Bogacz P, Kaczmarek J (2008) Study of flood embankment behaviour induced by air entrapment. In: Samuels P, Huntington S, Allsop W, Harrop J (eds) Flood risk management: research and practice. Taylor & Francis, London, pp 655–665
47. Lewis R, Schrefler B (1998) The finite element method in the static and dynamic deformation and consolidation of porous media. Wiley, Chichester
48. Lu N, Likos W (2004) Unsaturated soil mechanics. Wiley, Hoboken
49. Luckner L, van Genuchten M, Nielsen D (1989) A consistent set of parametric models for the two-phase flow of immiscible fluids in the subsurface. Water Resources Research 25(10):2113–2124,10.1029/WR025i010p02187

50. Morel-Seytoux H, Billica J (1985a) A two-phase numerical model for prediction of infiltration: applications to a semi-infinite soil column. Water Resources Research 21(4):607–615,10.1029/WR021i004p00607
51. Morel-Seytoux H, Billica J (1985b) A two-phase numerical model for prediction of infiltration: case of an impervious bottom. Water Resources Research 21(9):1389–1396,10.1029/WR021i009p01389
52. Mosthaf K, Baber K, Flemisch B, Helmig R, Leijnse T, Rybak I, Wohlmuth B (2011) A coupling concept for two-phase compositional porous-medium and single-phase compositional free flow. Water Resources Research 47:W10522,10.1029/2011WR010685
53. Mualem Y (1976) A new model for predicting the hydraulic conductivity of unsaturated porous media. Water Resources Research 12(3):513–522,10.1029/WR012i003p00513
54. Mualem Y (1978) Hydraulic conductivity of unsaturated porous media: Generalized macroscopic approach. Water Resources Research 14(2):325–334,10.1029/WR014i002p00325
55. Narasimhan T (2007) Central ideas of Buckingham (1907): A century later. Vadose Zone Journal 6(4):687–693,10.2136/vzj2007.0080
56. Niessner J, Hassanizadeh S (2008) A model for two-phase flow in porous media including fluid-fluid interfacial area. Water Resources Research 44:W08439,10.1029/2007WR006721
57. Oettl G, Stark R, Hofstetter G (2004) Numerical simulation of geotechnical problems based on a multi-phase finite element approach. Computers and Geotechnics 31(8):643–664,10.1016/j.compgeo.2004.10.002
58. Or D, Wraith J (2002) Soil water content and water potential relationships. Warrick A (ed) Soil physics companion, CRC Press, In, pp 49–84
59. Ossowski R, Sikora Z (2004) Numeryczne modelowanie sondowania statycznego CPTU (Numerical modeling of static CPTU tests). Politechnika Gdańska, Gdańsk
60. Parlange JY, Hill D (1979) Air and water movement in porous media: compressibility effects. Soil Science 127(5):257–263
61. Philip J (1969) Theory of infiltration. Advances in Hydroscience 5:215–296
62. Pinder G, Celia M (2006) Subsurface hydrology. Wiley, Hoboken
63. Pinder G, Gray W (2008) Essentials of multiphase flow and transport in porous media. Wiley, Hoboken
64. Radcliffe D, Šimunek J (2010) Soil physics with Hydrus. CRC Press, Boca Raton, Florida, Modeling and applications
65. Richards L (1931) Capillary conduction of liquids through porous medium. Physics 1:318–333
66. Rose W (2000) Myths about later-day extensions of Darcy's law. Journal of Petroleum Science and Engineering 26:187–198
67. Ross P (2003) Modeling soil water and solute transport—fast simplified numerical solutions. Agronomy Journal 95(6):1352–1361,10.2134/agronj2003.1352
68. Rucker D, Warrick A, Ferré T (2005) Parameter equivalence for the Gardner and van Genuchten soil hydraulic conductivity functions for steady vertical flow with inclusions. Advances in Water Resources 28(7):689–699,10.1016/j.advwatres.2005.01.004
69. Schaap M, Leij F (2000) Improved prediction of unsaturated hydraulic conductivity with the Mualem - van Geuchten model. Soil Science Society of America Journal 64(3):843–851,10.2136/sssaj2000.643843x
70. Sheng D, Sloan S, Gens A, Smith D (2003) Finite element formulation and algorithms for unsaturated soils. Part I: Theory. International Journal for Numerical and Analytical Methods in Geomechanics 27(9):745–765
71. Sikora Z (1992) Hypoplastic flow of granular materials - A numerical approach, vol 123. Veröffentlichungen des Institutes für Bodenmechanik und Felsmechanik der Universität Fridericiana in Karlsruhe, Karlsruhe
72. Šimunek J, Šejna M, Saito H, Sakai M, van Genuchten M (2008) The HYDRUS-1D software package for simulating the one-dimensional movement of water, heat and multiple solutes in variably-saturated media. Version 4.0. Department of Environmental Sciences, University of California Riverside, Riverside, California

73. Tegnander C (2001) Models for groundwater flow: A numerical comparison between Richards model and fractional flow model. Transport in Porous Media 43(2):213–224, 10.1023/A:1010749708294

74. Touma J, Vauclin M (1986) Experimental and numerical analysis of two-phase infiltration in a partially saturated soil. Transport in Porous Media 1(1):27–55, 10.1007/BF01036524

75. Touma J, Vachaud G, Parlange JY (1984) Air and water flow in a sealed, ponded vertical soil column: experiment and model. Soil Science 137(3):181–187

76. Vachaud G, Vauclin M, Khanji D, Wakil M (1973) Effects of air pressure on water flow in an unsaturated stratified vertical column of sand. Water Resources Research 9(1):160–173, 10.1029/WR009i001p00160

77. Valdes-Parada F, Ochoa-Tapia J, Alvarez-Ramirez J (2009) Validity of the permeability Carman-Kozeny equation: A volume averaging approach. Physica A 388(6):789–798

78. van Dijke M, van der Zee S (1998) Modeling of air sparging in a layered soil: Numerical and analytical approximations. Water Resources Research 34(3):341–353, 10.1029/97WR03069

79. van Genuchten M (1980) A closed form equation for predicting the hydraulic conductivity of unsaturated soils. Soil Science Society of America Journal 44(5):892–898, 10.2136/sssaj1980.03615995004400050002x

80. Vauclin M (1989) Flow of water and air in soils: theoretical and environmental aspects. In: Morel-Seytoux H (ed) Unsaturated flow in hydrologic modeling: theory and practice. Kluwer, Dordrecht

81. Vogel T, Císlerová M (1988) On the reliability of unsaturated hydraulic conductivity calculated from the moisture retention curve. Transport in Porous Media 3(1):1–15, 10.1007/BF00222683

82. Vuković M, Soro A (1992) Determination of Hydraulic Conductivity of Porous Media from Grain-Size Composition. Water Resources Publications, Litleton, Colorado

83. Wang Z, Feyen J, Nielsen D, van Genuchten M (1997) Two-phase flow infiltration equations accounting for air entrapment effects. Water Resources Research 33(12):2759–2767, 10.1029/97WR01708

84. Wang Z, Feyen J, van Genuchten M, Nielsen D (1998) Air entrapment effects on infiltration rate and flow instability. Water Resources Research 34(2):213–222, 10.1029/97WR02804

85. Warrick A (2003) Soil water dynamics. Oxford University Press, New York

86. Whitaker S (1986) Flow in porous media I: A theoretical derivation of Darcy's law. Transport in Porous Media 1(1):3–25, 10.1007/BF01036523

87. Wu Y, Forsyth P, Jiang H (1996) A consistent approach for applying numerical boundary conditions for multiphase subsurface flow. Journal of Contaminant Hydrology 23(3):157–184, 10.1016/0169-7722(95)00099--2

88. Yazzan S, Bentsen R, Trivedi J (2011) Theoretical development of a novel equation for dynamic spontaneous imbibition with variable inlet saturation and interfacial coupling effects. Transport in Porous Media 86(3):705–717, 10.1007/s11242-010-9647-z